

## RESEARCH ARTICLE

# An immune response to the avascular lens following wounding of the cornea involves ciliary zonule fibrils

JodiRae DeDreu<sup>1</sup> | Caitlin J. Bowen<sup>1</sup> | Caitlin M. Logan<sup>1</sup> | Sonali Pal-Ghosh<sup>2</sup> | Paola Parlanti<sup>3</sup> | Mary Ann Stepp<sup>2,4</sup> | A. Sue Menko<sup>1,5</sup>

<sup>1</sup>Department of Pathology, Anatomy and Cell Biology, Sidney Kimmel Medical College, Thomas Jefferson University, Philadelphia, PA, USA

<sup>2</sup>Department of Anatomy and Cell Biology, George Washington University School of Medicine and Health Sciences, Washington, DC, USA

<sup>3</sup>George Washington University Nanofabrication and Imaging Center, George Washington University School of Medicine and Health Sciences, Washington, DC, USA

<sup>4</sup>Department of Ophthalmology, George Washington University School of Medicine and Health Sciences, Washington, DC, USA

<sup>5</sup>Department of Ophthalmology, Sidney Kimmel Medical College, Thomas Jefferson University, Philadelphia, PA, USA

## Correspondence

A. Sue Menko, Department of Pathology, Anatomy and Cell Biology, Co-Director, Wills Vision Research Center at Jefferson, Thomas Jefferson University, 564 Jefferson Alumni Hall, 1020 Locust Street, Philadelphia, PA 19107, USA.  
Email: sue.menko@jefferson.edu

## Funding information

HHS | NIH | National Eye Institute (NEI), Grant/Award Number: EY021784

## Abstract

The lens and central cornea are avascular. It was assumed that the adult lens had no source of immune cells and that the basement membrane capsule surrounding the lens was a barrier to immune cell migration. Yet, microfibril-associated protein-1 (MAGP1)-rich ciliary zonules that originate from the vasculature-rich ciliary body and extend along the surface of the lens capsule, form a potential conduit for immune cells to the lens. In response to cornea debridement wounding, we find increased expression of MAGP1 throughout the central corneal stroma. The immune cells that populate this typically avascular region after wounding closely associate with this MAGP1-rich matrix. These results suggest that MAGP1-rich microfibrils support immune cell migration post-injury. Using this cornea wound model, we investigated whether there is an immune response to the lens following cornea injury involving the lens-associated MAGP1-rich ciliary zonules. Our results provide the first evidence that following corneal wounding immune cells are activated to travel along zonule fibers that extend anteriorly along the equatorial surface of the lens, from where they migrate across the anterior lens capsule. These results demonstrate that lens-associated ciliary zonules are directly involved in the lens immune response and suggest the ciliary body as a source of immune cells to the avascular lens.

**Abbreviations:** DAMPs, damage-associated molecular patterns; ECM, extracellular matrix; HA, hyaluronic acid; LTBP, latent transforming growth factor  $\beta$ 1 binding proteins; LYVE-1, lymphatic vessel endothelial hyaluronan receptor-1; MAGP1, microfibril-associated protein-1 (MAGP1); N-cad<sup>Δlens</sup>, lens-conditional embryonic knockout of N-cadherin; NETs, neutrophil extracellular traps; PCO, Posterior Capsule Opacification; TGF $\beta$ , Transforming Growth Factor  $\beta$ ; TLR4, toll-like receptor 4; TN-C, tenascin-C; TSP-1, thrombospondin-1.

This is an open access article under the terms of the Creative Commons Attribution-NonCommercial License, which permits use, distribution and reproduction in any medium, provided the original work is properly cited and is not used for commercial purposes.

© 2020 The Authors. The FASEB Journal published by Wiley Periodicals LLC on behalf of Federation of American Societies for Experimental Biology

## KEYWORDS

cornea wounding, ciliary zonules, immune response, lens

## 1 | INTRODUCTION

The anterior segment of the eye, long been considered immune privileged, now must instead be considered immune tolerant, having adapted novel mechanisms to provide immune cell responses in the absence of a vasculature. Our previous studies of a lens-conditional embryonic knockout of N-cadherin (N-cad<sup>Δlens</sup>) provided the first evidence that immune cells are recruited to the avascular lens, in this case in response to lens dysgenesis.<sup>1</sup> The earliest immune cells detected within these dysgenic lenses are macrophages, followed by B cells and T cells,<sup>1</sup> evidence that an adaptive immune response can be activated by lens pathologies, and that immune cells can populate the lens. The morphogenetic defects that begin during the development of the N-cad<sup>Δlens</sup> mouse lens<sup>2</sup> result in more severe lens dysgenesis in the adult resulting in cataract-like opacities.<sup>1</sup> In adult mice, the immune cells that are recruited to these dysgenic lenses acquire a myofibroblast phenotype prior to the development of cataracts.<sup>1</sup> Myofibroblasts, such as those that appear in these dysgenic lenses and the collagen I matrix they produce have long been associated with lens fibrotic pathologies, including cataracts. These studies provided evidence that immune cells that associated with the lens need to be considered as potential agents of lens disease.

During mammalian development the lens is surrounded by a fetal vasculature,<sup>3,4</sup> a potential source of resident immune cells of the lens, including the F4/80+ macrophages that associate with the mouse lens primordium.<sup>5</sup> In those early studies, F4/80+ were not detected at later stages of development. The lens-associated vasculature, an anastomosed network of the tunica vasculosa lentis originating from the hyaloid artery, and the anterior pupillary membrane, which extends from the ciliary veins, regresses around the time of birth via programmed cell death.<sup>6,7</sup> Its failure to involute results in Persistent Fetal Vasculature Syndrome and visual impairment. Therefore, it has been believed that there are no sources of immune cells to protect or repair the lens after birth. Our previous studies with N-cad<sup>Δlens</sup> mice that showed immune cells are recruited to dysgenic lenses in adult mice,<sup>1</sup> and demonstrate the capability to activate an adaptive immune response in the adult lens.

Multiple sites within the eye have been previously shown to harbor innate immune cells, including the uvea, composed of the iris, choroid, and ciliary body, as well as the cornea and conjunctiva,<sup>8,9</sup> while the retina has been shown to contain myeloid cells, similar to brain microglia.<sup>10</sup> Additionally, while the intraocular compartments lack traditional lymphatics,

aqueous fluid drains via episcleral blood vessels to reach traditional immune organs including the spleen and thymus.<sup>11</sup> There also exists an eye-draining lymph node, designed to receive antigenic material from the eye<sup>12-14</sup> and previous reports indicate that in pathogenic conditions, lymphatics can be induced in the cornea<sup>15,16</sup> and likely in the uveal tissues<sup>17,18</sup> that would allow for a rapid immunologic response. Previous research has also demonstrated that the aqueous humor is capable of inducing regulatory T cells to produce Transforming Growth Factor  $\beta$  (TGF $\beta$ ).<sup>19,20</sup> This TGF $\beta$  pathway has been thought in part to regulate dendritic cells present in the aqueous humor to mediate immune tolerance in the anterior chamber.<sup>21,22</sup> Additionally, in disease states such as glaucoma, the aqueous humor has also been populated by antibodies including those against  $\alpha$ B crystallin and vimentin.<sup>23,24</sup> The innate immune cells of the eye, in addition to the circulatory system of the eye's vasculature and aqueous humor drainage, likely work in tandem to regulate immune response to the lens.

Additionally, our prior studies showed evidence that in the case of lens dysgenesis, lens-associated immune cells likely transit by way of the fibrillin-rich ciliary zonules,<sup>1</sup> structures that connect the ciliary body to the lens.<sup>25-27</sup> The ciliary zonules are produced by the nonpigmented ciliary epithelial cells of the ciliary body.<sup>28</sup> While the primary role of the ciliary zonules is to transmit contractile forces from the smooth muscle of the ciliary body integral to lens function of focusing images on the retina, a process referred to as accommodation, the zonule proteome includes numerous extracellular matrix (ECM) and signaling proteins that can provide an environment permissive for cell migration. These potential pro-migratory molecules include fibrillin-1, fibrillin-2, latent transforming growth factor  $\beta$ 1 binding proteins (LTBPs), and Microfibril-Associated Glycoprotein-1 (MAGP1),<sup>29</sup> a fibrillin-binding protein that sequesters and regulates the release of active forms of TGF $\beta$ .<sup>30</sup> Other zonule components that could participate in directing immune cell migration include matricellular proteins like tenascin-C (TN-C) and thrombospondin-1 (TSP-1). TN-C supports immune cell adhesion through its binding of the toll-like receptor (TLR4).<sup>31,32</sup> TSP-1 is involved in the activation of latent TGF $\beta$ ,<sup>33,34</sup> and TSP-1 functions as an integrin ligand,<sup>35</sup> both which may be responsible for the role of TSP-1 in immune cell migration.<sup>36</sup>

The hyaluronic acid (HA) receptor lymphatic vessel endothelial hyaluronan receptor-1 (LYVE-1) is expressed by immune cells and lymphatic endothelial cells.<sup>17,37-39</sup> Its extracellular domain, which is shed from the surface of activated immune cells,<sup>40,41</sup> co-localizes with MAGP-1 along the

ciliary zonules,<sup>1</sup> where it is likely left behind by immune cells traveling between the vasculature of the ciliary body and the lens. Cleavage of LYVE-1 could be executed by proteases known to be associated with the zonules<sup>29</sup> or secreted by the immune cells themselves. The association of the LYVE-1 ectodomain with the ciliary zonules is enhanced in the eyes of adult N-cad<sup>Δlens</sup> mice, a finding consistent with increased transit of immune cells along the zonules to populate these dysgenic lenses.<sup>1</sup>

We have now conducted studies to investigate whether there are mechanisms that provide an immune cell response to the avascular lens. Since our studies of adult N-cad<sup>Δlens</sup> mice revealed that there is an immune response throughout avascular regions of the eye to the dysgenesis of the lens,<sup>1</sup> we now examined whether immune cells were activated to surveil the lens in response to inflammatory cues arising from cornea debridement wounding. With these studies, we discovered that within 1 day of corneal wounding there is active recruitment of immune cells to the lens, with immune cells populating the ciliary zonules along the equatorial and anterior surfaces of the lens. From their position within the zonules on the lens surface, these immune cells are able to migrate across the lens capsule. As we previously found that immune cells recruited to the dysgenic lenses of adult N-cad<sup>Δlens</sup> mice acquire a myofibroblast phenotype prior to the development of cataract-like opacities,<sup>1</sup> our new findings also suggest that immune cells that are induced to associate with the lens in response to injury or disease in other regions of the eye may become the cause of lens fibrotic pathologies.

## 2 | MATERIALS AND METHODS

### 2.1 | Animals

All animal studies performed were approved by the George Washington University Medical Center Institutional Animal Care and Use Committee (IACUC) and the Thomas Jefferson University IACUC. These studies comply with all relevant guidelines. In addition, they comply with the Association for Research in Vision and Ophthalmology (ARVO) Statement for the Use of Animals in Ophthalmic and Vision Research (<https://www.arvo.org/About/policies/statement-for-the-use-of-animals-in-ophthalmic-and-vision-research>).

7w-8w Male BALB/c mice from Charles River at Frederick MD were used for mouse cornea wounding experiments and for unwounded control mice. Debridement wounding was performed as described previously.<sup>42</sup> In brief, mice were anesthetized with ketamine/xylazine and a topical anesthetic applied to their ocular surface. A 2.5 mm trephine was used to demarcate the wound area and

the epithelial cells within a 2.5 mm trephine area were removed using a dulled blade. Wounding was bilateral. After wounding, erythromycin ophthalmic ointment was applied to the injured cornea and mice were allowed to heal for 1 day, and then, euthanized.

### 2.2 | Immunofluorescence labeling

For immunolabeling studies of mouse eyes, whole mouse eyes were removed immediately after euthanasia, fixed overnight at 4°C in 3.7% of paraformaldehyde, washed in PBS, cryoprotected in 30% of sucrose, and frozen in OCT. 20 μm thick cryosections were cut. Sections were permeabilized (0.5% Triton X100 in DPBS [2.7 mM KCl, 1.5 mM KH<sub>2</sub>PO<sub>4</sub>, 137.9 mM NaCl, 8.1 mM Na<sub>2</sub>HPO<sub>4</sub>·7H<sub>2</sub>O] [Corning]) for 1 hour, incubated in block buffer (5% goat/donkey serum, 3% bovine serum albumin [BSA] in DPBS, 0.25% Triton X100) for 2 hours, incubated in primary antibody diluted in block buffer overnight at 37°C, washed, and then, incubated for 1 hour in secondary antibody (Jackson ImmunoResearch Laboratories) diluted in block buffer. Primary antibodies used included MAGP1 (gift, R. Mecham, Washington University, St. Louis), Perlecan (Santa Cruz, SC-33707), TSP-1 (Santa Cruz, SC-393504), GR1 (Ly-6G/Ly-6C, Biolegend, 108448), CD45 (Biolegend, 103122), CD68 (Biolegend, 137012), and Laminin (Sigma Aldrich, L9393). F-actin was labeled with fluorescent-conjugated phalloidin (Invitrogen, A12381 or A22284), and nuclei were with labeled with DAPI (Biolegend, 422801) or TO-PRO-3 (Invitrogen).

For immunolabeling of mouse lens whole mounts, whole eyes were fixed as above, the lenses removed after making a cut in the back of the eye, washed two times for 30 minutes, and incubated in blocking buffer (1% BSA in PBS) with gentle shaking at room temperature for 10 minutes. A 1% of horse serum was added to the block buffer and incubated for an additional minute. Lenses were incubated overnight at 4°C with MAGP1 antibody (gift, R. Mecham) diluted in blocking buffer, washed five times for 1 hour with PBS and 0.02% Tween 20 (PBST), blocked for 2 hours, and then, incubated with secondary antibody (DyLite 488, Jackson Immunobiologicals) diluted in blocking buffer overnight at 4°C. Lenses were costained with phalloidin (Invitrogen), washed three times for 1 hour with PBST, and placed on indented slides that were covered with mounting media (Fluoromount G; Electron Microscopy Sciences) prior to coverslipping.

### 2.3 | Scanning electron microscopy

Lenses were fixed in 2.5% of glutaraldehyde and 1% of paraformaldehyde in sodium cacodylate buffer. After rinsing, the

samples were postfixed in 1% of osmium tetroxide. A serial dehydration in ethyl alcohol was followed by critical point drying (Autosamdri-931, Tousimis, Rockville, MD). A thin layer of gold was sputtered onto the surface of the samples (Cressington 208HR, Ted Pella Inc, Redding, CA) before imaging in the FEI Teneo LV Scanning Electron Microscope (Thermo Fisher, Hillsboro, OR). Imaging conditions were 2.0 KV with a working distance of 8.7 mm using the Everhart Thornley detector.

## 2.4 | Image analysis

Images of immunolabeled samples were examined using a Zeiss LSM800 confocal microscope. When indicated, super-resolution images were acquired using the Airyscan feature on the Zeiss LSM800. Z-stacks with 1  $\mu\text{m}$  optical sections were collected and analyzed using Zeiss Zen software and 3D images were created using Imaris software (Version 9.5). Imaging of mouse lens whole mounts was performed with a Zeiss 710 confocal microscope. Z-stacks with 1  $\mu\text{m}$  optical sections were acquired and 3D images created either with Imaris software (Version 9.5) or Volocity software (Version 6.3, Perkin Elmer).

## 2.5 | Statistics

For quantification data, eyes from wounded and unwounded animals were imaged using Zeiss LSM800 and individual CD45+ immune cells were counted in specific regions of the eye: ciliary body, equatorial zone of the lens, and anterior epithelium area of the lens. Data represent mean  $\pm$  SD and a *t* test was performed to compare wounded and unwounded samples, with a *P* < .05 being considered significant.

# 3 | RESULTS

## 3.1 | Elastic fibril-associated MAGP1 and TSP-1 in normal and corneal wounded eyes

Following corneal debridement wounding (Figure 1A), immune cells migrate to the avascular region of the central cornea from the limbal blood vessels. They move through the corneal stromal matrix, which is comprised primarily of collagens and proteoglycans organized into lamellae.<sup>43</sup> Fibrillin is a structural component of the elastic fibers of the cornea stroma.<sup>44,45</sup> Also the backbone of the ciliary zonules, fibrillin provides the molecular site for binding of MAGP1.<sup>25,26,29</sup> Confocal imaging of cryosections of unwounded mouse eyes immunolabeled for MAGP1 revealed a distinctive distribution within the normal cornea stroma where it localizes to

the matrix between stromal lamellae and is most abundant at the anterior aspect Descemet's membrane (Figure 1B), the same region that is enriched for fibrillin and elastic fibers. By contrast, MAGP1 is rarely detected in the corneal stroma adjacent to the epithelial basement membrane (Figure 1B). To the best of our knowledge, the presence of MAGP1 in adult corneas had not been previously investigated.

Immunolocalization studies show that both the expression and distribution of MAGP1 increased throughout the stroma within 1 day of cornea debridement wounding (Figure 1C). The absence of the epithelial barrier resulted in swelling of the corneal stroma during fixation of the tissue; stromal swelling is not seen at the corneal periphery where the epithelium is present after wounding. Remaining localized to the stroma above Descemet's membrane, in response to wounding MAGP1 becomes uniformly distributed throughout the corneal stroma (Figure 1C). The MAGP1 staining pattern within the stroma reveals that this protein co-localizes with collagen lamellae; the intense puncta seen in both the control and wounded corneas suggests that MAGP1 also associates with proteoglycans. As previously reported,<sup>46,47</sup> and paralleling the increase in MAGP1, TSP-1 is greatly increased in the corneal stroma at 1D post-corneal wounding (Figure 1D,E).

## 3.2 | Association of migrating immune cells with MAGP1-rich microfibrils in the central corneal stroma following debridement wounding

To maintain transparency, blood and lymphatic vessels are excluded from the light path in the cornea. The immune cells that populate the cornea before and after injury derive from cells in the peripheral limbal vasculature, the aqueous humor, and the tears.<sup>48,49</sup> Our labs and others have shown that innate immune cells rapidly populate the central cornea in response to corneal injury.<sup>50-52</sup> Here, we have extended these findings to show the close association between immune cells and MAGP1-rich microfibrils in unwounded corneas and in corneas at 1 day following debridement wounding (Figure 2). Cryosections were co-immunolabeled for MAGP1 and CD45, a surface protein expressed by immune cells that we have used previously to show immune cells at the wound edge following corneal debridement wounding.<sup>50-52</sup> In unwounded corneas, immune cells are present in both the peripheral cornea (Figure 2A-C) and in the limbal region (Figure 2G-I). An influx and increase in immune cells was observed in both regions at 1 day post-injury (Figure 2D-F,J-L), particularly in the limbal region, consistent with prior studies of the involvement of this area in immune response.<sup>53,54</sup> In both wounded and unwounded corneas, CD45+ immune cells are seen transiting through a MAGP1-rich matrix with a close association between



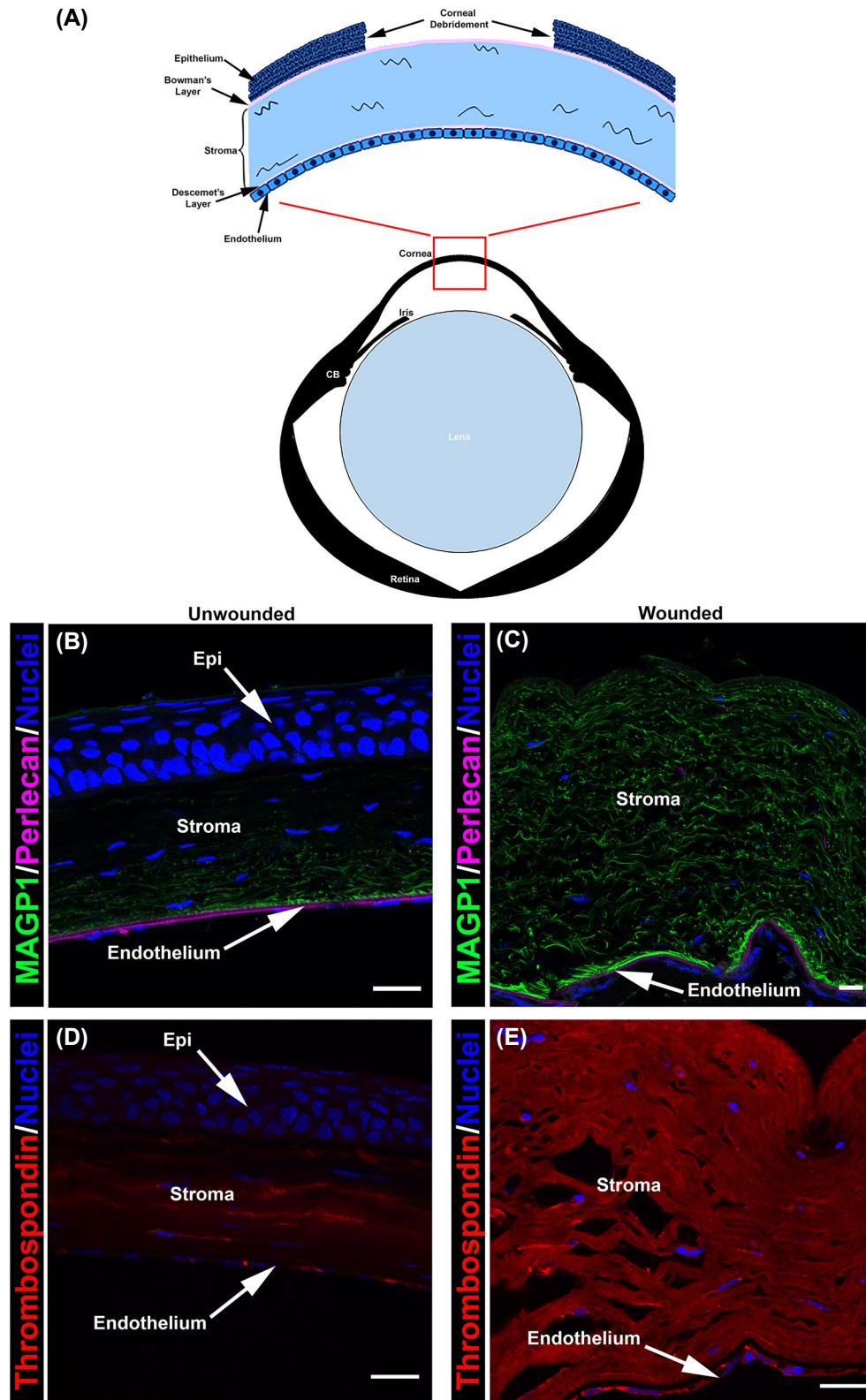
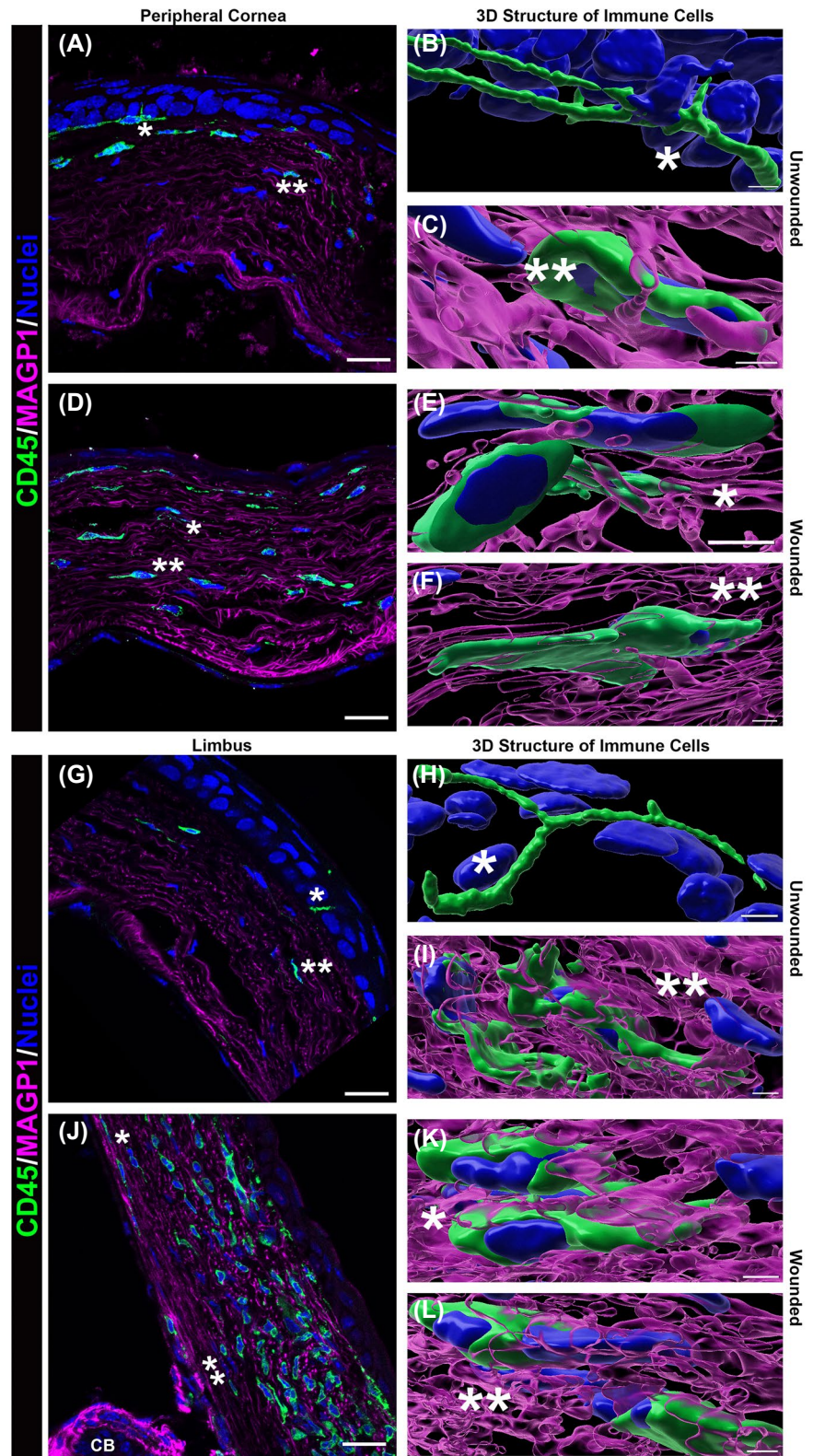


**FIGURE 1** Upregulation of elastic-fibril-associated MAGP1 and Thrombospondin in response to corneal debridement injury. A, Model of corneal debridement wounding; wavy lines denote stromal cells. B-E, Central cornea region of whole mouse eye cryosections; (B,D) unwounded and (C,E) 1 day post-corneal debridement wounding. B and C, Co-immunolabeled for MAGP1 (green) and perlecan (purple) and labeled for nuclei (blue). D and E, Labeled for thrombospondin (red) and nuclei (blue). In unwounded eyes MAGP1 is most abundant in the stroma adjacent to Descemet's membrane and becomes uniformly distributed throughout the corneal stroma by 1D post-wounding. Like MAGP1, expression of thrombospondin in the uninjured cornea is low and greatly increased in the corneal stroma at 1D post-corneal wounding. Studies are representative of at least three independent experiments. Magnification bars = 20  $\mu$ m. Epi = corneal epithelium

**FIGURE 2** Immune cells locate along MAGP1-rich fibrils in the stroma following corneal debridement wounding. Cryosections of whole mouse eyes, both (A-C, G-I) unwounded and (D-F, J-L) at 1 day post-corneal debridement wounding, imaged at (A-F) the peripheral cornea and (G-L) the limbus. All sections were co-immunolabeled for MAGP1 (purple) with immune cell marker CD45 (green) and nuclei (blue). (B,C,E,F,H,I,K,L) are 3D structural images created with Imaris software from confocal Z-stacks. Asterisks indicate the same cells in different images. Immune cells increase in the peripheral cornea and limbus and are closely associated with MAGP1 fibrils. Studies are representative of at least three independent experiments. Magnification bars = 20  $\mu\text{m}$  in A,D,G,J; = 4  $\mu\text{m}$  in B; = 2  $\mu\text{m}$  in C,F,I,K,L; = 3  $\mu\text{m}$  in E; 5  $\mu\text{m}$  in H



MAGP1 and these cells highlighted in 3D structural representations of confocal Z-stacks (Figure 2B,C,E,F,H,I,K,L), suggesting a role for MAGP1 in immune cell migration through the cornea stroma.

To further investigate the immune response to corneal debridement, we looked for the presence of a variety of

immune cell types and their association with MAGP1 in the region of the corneal debridement wound, which spans the central cornea. CD68 preferentially labels a surface protein on macrophages/monocytes, and GR1 recognizes LY6G/LY6C, a myeloid differentiation antigen used to detect neutrophils. For these studies, wounded corneas were imaged



in both the central region debrided of the epithelium and in the region of the epithelial wound edge. Unwounded corneas, imaged spanning both these regions, have few detectable immune cells (Figure 3A,D,G), as shown previously. In response to cornea debridement wounding, CD45+ immune cells (Figure 3B,C), including CD68+ macrophage/monocytes (Figure 3E,F) and GR1+ neutrophils (Figure 3H,I), populate the corneal stroma beneath the epithelial wound edge and have even migrated into the central cornea stroma where the epithelial barrier is absent. Immune cells are more abundant in the anterior stroma where MAGP1 is expressed post-wounding and again we see these cells in close association with MAGP1-rich microfibrils. Immune cells increase in the central cornea stroma at the same time points that MAGP1 expression increases, showing a positive correlation between their presence.

### 3.3 | MAGP1 and TSP-1 are highly-associated with the ciliary zonules in normal and corneal wounded eyes

We also compared the expression and distribution of MAGP1 and TSP-1 in the ciliary zonules of unwounded and corneal-wounded adult mouse eyes. As reported previously,<sup>25,26,29</sup> the ciliary zonules linking the ciliary body to the lens in normal eyes (modeled, Figure 4A) are rich in the fibrillin-binding protein MAGP1 (Figure 4B). The zonule fibers first contact the lens capsule at its equator from where a subset extends along the surface of the lens in both anterior and posterior directions in both unwounded and corneal wounded eyes (Figures 4B,C and 5A).<sup>25,55</sup> The MAGP1-rich anterior-directed zonule microfibrils are closely linked to the superficial surface of the lens equatorial capsule, reaching as far as the uppermost region of the lens equatorial zone (Figure 5B,C). No MAGP1+ ciliary zonules fibers were detected along the anterior surface of the lens capsule before or after corneal wounding (Figure 5D,F). Here, the lens capsule surface is rich in basement membrane proteins like perlecan (Figure 5E,G) and laminin (Figure 6B). We now find that in contrast to the corneal stroma, high levels of TSP-1 are associated with the ciliary zonules of unwounded eyes (Figure 4D), and that TSP-1 is also associated with the superficial surface of the anterior lens capsule (Figure 6A,C). Already highly expressed prior to wounding, the association of MAGP1 and TSP-1 with the ciliary zonules is not significantly increased following corneal wounding (Figure 4C,E). Our finding that the avascular ciliary zonules of adult, mammalian eyes are rich in TSP-1 as well as MAGP1 is consistent with a function for these molecules in providing a microenvironment that promotes the migration of immune cells between the vasculature-rich ciliary body and the surface of the lens.

### 3.4 | A role for the ciliary zonules in the immune cell response to the avascular lens upon injury to the cornea

A protective immune response of the lens following cornea debridement wounding would be expected to result in immune cells being associated with the surface of the lens, possibly having traveled along the ciliary zonule fibers. We investigated the possibility that the lens-surface associated ciliary zonule fibers provide a mechanism by which immune cells can surveille the lens in response to injury to the cornea. Cryosections of adult eyes, both unwounded and at 1 day post-corneal debridement wounding, were immunolabeled for the leukocyte common antigen CD45 and co-immunolabeled for the ciliary zonule protein MAGP1 (Figure 7). Confocal imaging was performed along the ciliary zonules between the ciliary body and the lens including the zonule fibers that extend along the equatorial surface of the lens capsule (Figure 7A-D). In unwounded lenses, CD45+ cells were present along the MAGP1-rich ciliary zonules between the ciliary body and the lens (Figure 7A). 3D structural imaging highlights the relationship between an immune cell in this region and MAGP1 (Figure 7C). Notably, no CD45+ cells were detected associated with the ciliary zonule fibers extended along the equatorial surface of the lens in unwounded eyes (Figure 7A). However, in response to corneal debridement wounding, CD45+ immune cells are induced to migrate in an anterior direction along the MAGP1+ zonule fibers extended along the surface of the perlecan-rich equatorial lens capsule (Figure 7B). When viewed as a 3D structural image, the close association of these CD45+ immune cells with the ciliary zonules extended along the perlecan-rich lens capsule is revealed (Figure 7D).

The immune response induced for protection of the lens when the cornea is wounded would be expected to involve movement of immune cells around the lens, beyond the region where the zonule fibrils end in the anterior-most region of the lens equator. To examine this possibility, we imaged the anterior surface of lenses following immunolabeling for CD45+ in unwounded eyes (Figure 7E) and in eyes at 1 day post-corneal debridement wounding (Figure 7F). No CD45+ cells were ever detected along the anterior surface of lenses in unwounded eyes (Figure 7E). However, in response to corneal wounding, CD45+ cells become localized all along the upper half of the lens, associated with the ciliary zonule fibrils extended anteriorly along the lens capsule equatorial surface (Figure 7B,D), as well as directly with the lens capsule along the anterior surface of the lens (Figure 7F). While MAGP1+ zonule fibers do not extend to the anterior-most region of the adult lens (Figure 5D,F), TSP-1 (Figure 6A,C), perlecan (Figures 5E,G and 7E), and laminin (Figure 6B,C) are expressed at the superficial surface of the anterior lens

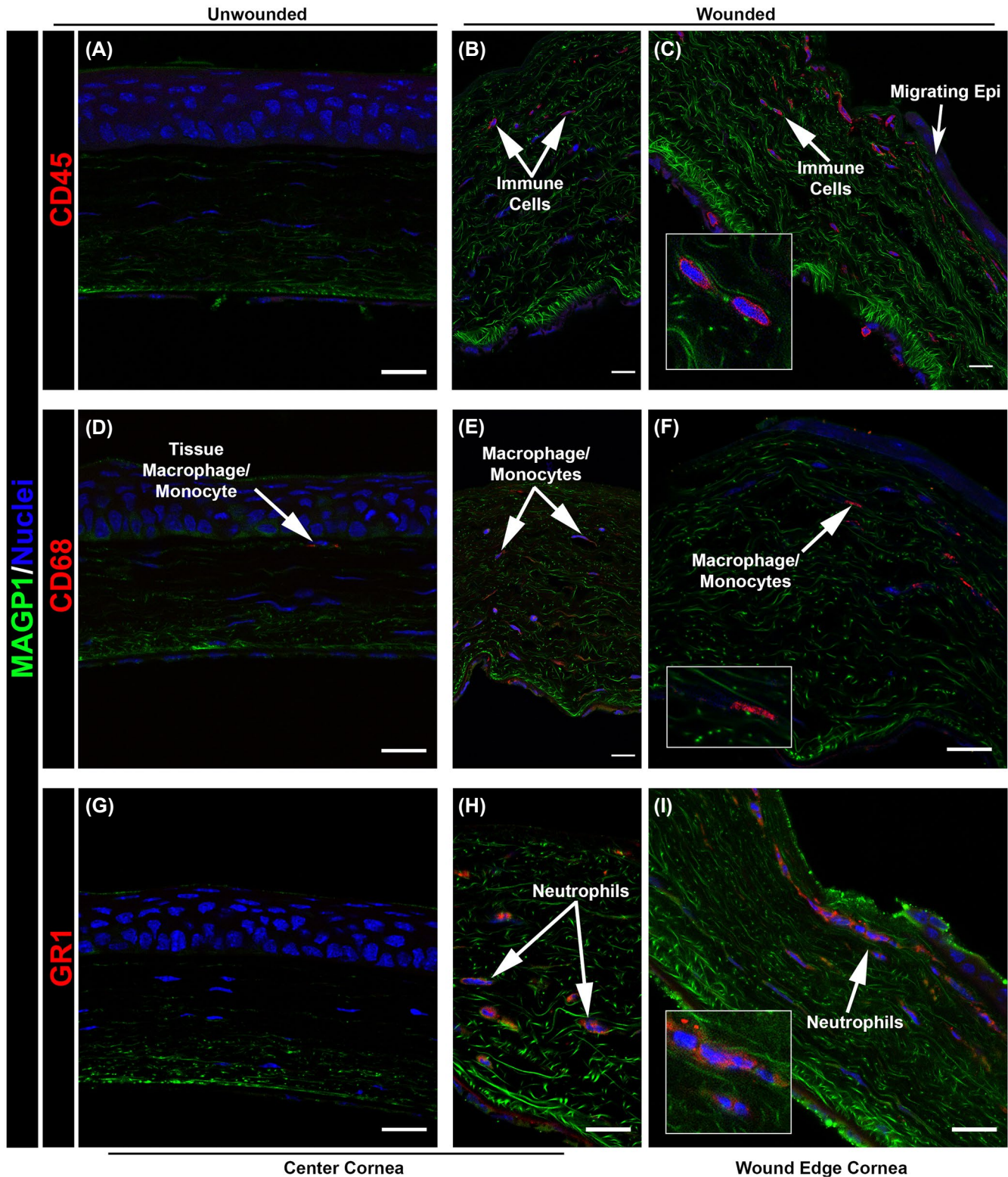


**FIGURE 3** Macrophages and leukocytes locate along MAGP1-rich fibrils in the stroma following corneal debridement wounding. Cryosections of whole mouse eyes, both (A,D,G) unwounded and (B,C,E,F,H,I) at 1 day post-corneal debridement wounding, imaged at (A,B,D,E,G,H) the central cornea and (C,F,I) the wound edge. Co-immunolabeling of (A-I) MAGP1 (green) with immune cell markers (A-C) CD45, (D-F) CD68, and (G-I) GR1. Nuclei labeled blue. While immune cells were rarely detected in the stroma of the central cornea of unwounded eyes, at 1D post-corneal wounding CD45+, CD68+, and GR1+ immune cells appeared to migrate along MAGP1-rich fibrils in the stroma of the central cornea and near the wound edge. Insets in C,F,I are high magnification views. Studies are representative of at least three independent experiments. Magnification bars = 20  $\mu$ m. Migrating Epi = Migrating Corneal Epithelium



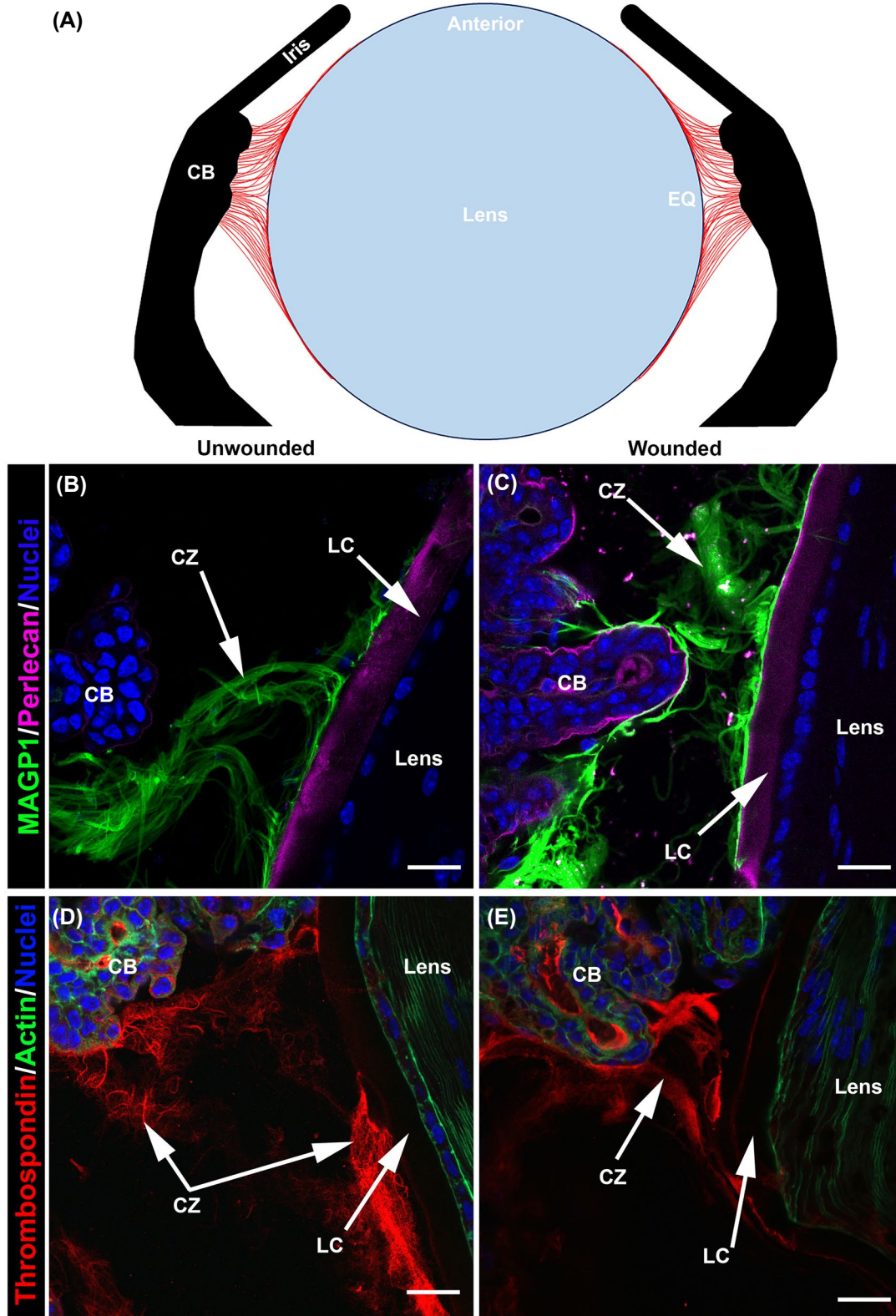


**FIGURE 4** Association of MAGP1 and thrombospondin rich ciliary zonules with the lens in normal and corneal wounded eyes. A, Model of ciliary zonules (red) linking the lens to the ciliary body. B-E, Whole mouse eye cryosections imaged between the ciliary body and the lens. B and D, unwounded eyes and (C,E) at 1 day post-corneal debridement wounding. B and C, Co-immunolabeling for MAGP1 (green) and perlecan (purple), also labeled for nuclei (blue). D and E, Immunolabeled for thrombospondin (red) and co-labeled for F-actin (green) and nuclei (blue). MAGP1 is highly associated with the ciliary zonules located between the ciliary body and the equator of the lens, as well as the zonule fibrils that extend along the lens surface for a short distance from the equator toward both its anterior and posterior poles. Association of MAGP1 and thrombospondin with the ciliary zonules was similar in unwounded and corneal wounded eyes. Studies are representative of at least three independent experiments. Magnification bars = 20  $\mu\text{m}$ . CB, ciliary body; CZ, ciliary zonules; LC, lens capsule

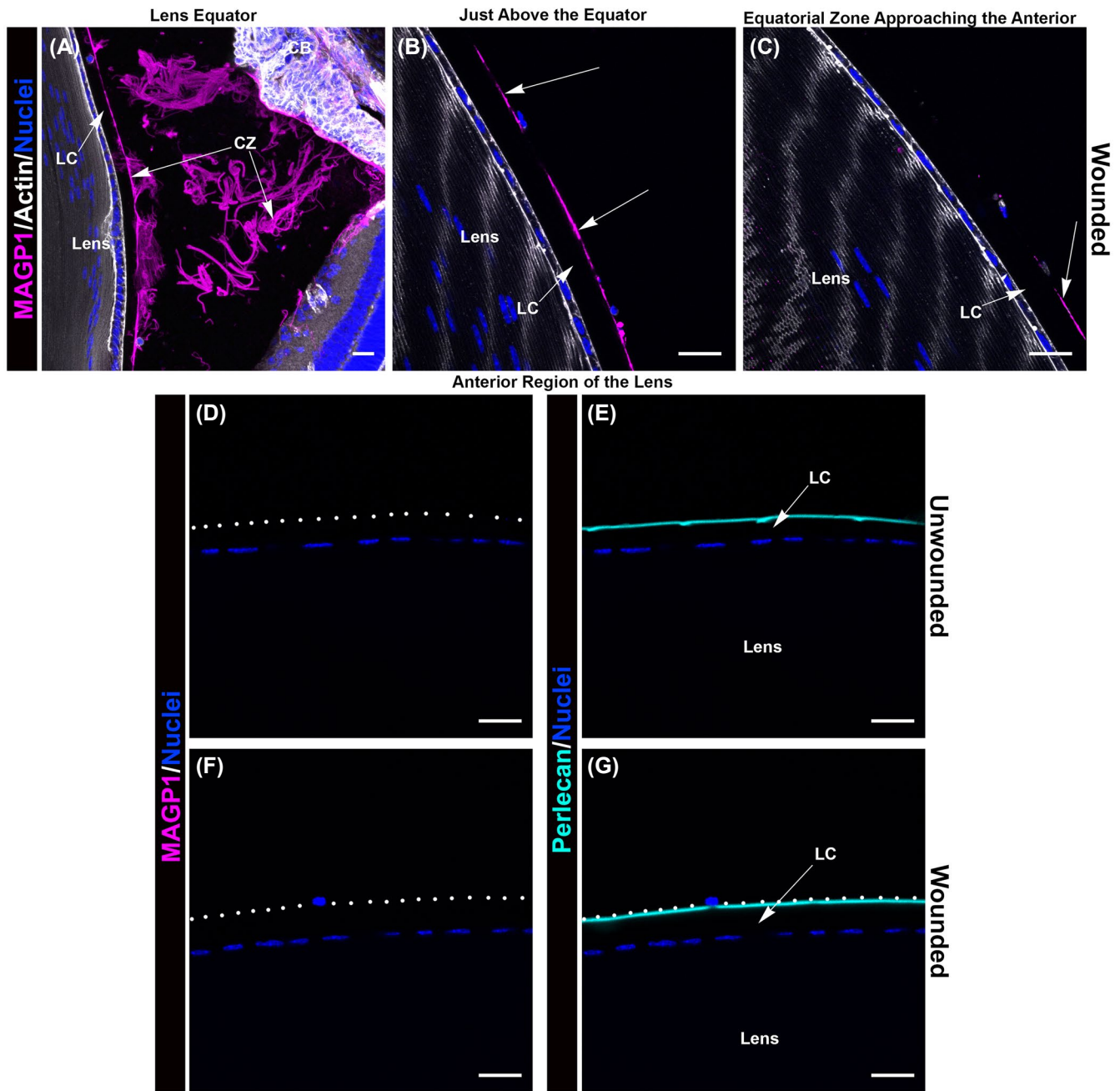


**FIGURE 5** Extension of MAGP1-rich microfibrils along the surface of the lens. A-C, Immunolabeling of ciliary zonule microfibrils with antibody to MAGP1 (purple) at 1 day post-corneal debridement wounding in sections co-labeled for F-actin (white) and nuclei (blue), (A) at the lens equator where the ciliary zonules (CZ) emanating from the ciliary body (CB) link to the lens capsule, (B) along the lens capsule (LC) just above the equator, and (C) higher up along the lens equatorial zone approaching the lens anterior, the region where the lens-associated zonule fibers terminate. D-G, The anterior region of the lens in (D,E) unwounded eyes and (F,G) at 1 day post-corneal debridement wounding, co-immunolabeled for (D,F) MAGP1 (purple) and (E,G) perlecan (green), also labeled for nuclei (blue). Dotted line in D,F,G represents the surface of the lens capsule (LC)

capsule. Together, these findings provide the first evidence that an immune response is activated that provides immune cells to surveil the lens when there is wounding of the cornea, with immune cells first migrating within MAGP1-rich microfibrils along the equatorial surface of the lens, and then, likely moving from the tips of these zonule structures to populate the anterior surface of the lens.

To further examine this immune response and immune cell trafficking following corneal wounding, we quantified the number of CD45+ immune cells present in three regions of wounded and unwounded eyes: the ciliary body, the lens equatorial surface, and the lens anterior surface (Figure 7G). We found a statistically significant increase in the number of immune cells present in all three regions at

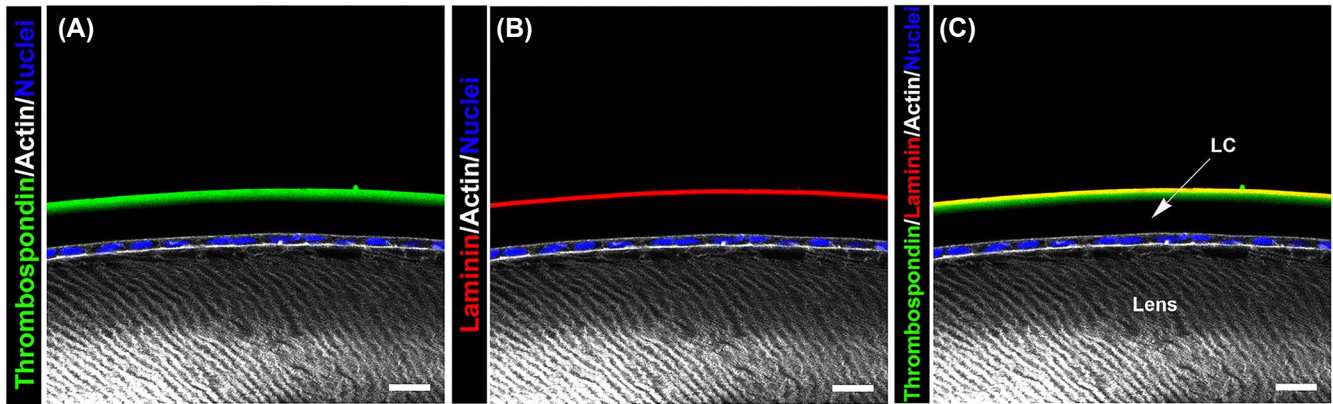


**FIGURE 6** Thrombospondin is localized to the superficial surface of the anterior lens capsule. Co-immunolabeling along the anterior lens surface of unwounded eyes for (A) thrombospondin (green) and (B) laminin (red), co-labeled for F-actin (white), and nuclei (blue), with (C) the thrombospondin and laminin overlay. Thrombospondin and laminin overlap at the superficial surface of the anterior lens capsule, thrombospondin extending just beyond laminin

1 day post-corneal wounding compared to unwounded controls (Figure 7G). This demonstrated that there was increased presence of CD45+ immune cells in the ciliary body in response to wounding in addition to increased transit of immune cells along the surface of the lens capsule toward the anterior epithelium.

### 3.5 | Immune cell subtypes that survey the lens in response to corneal wounding

To further identify the immune cells that are activated to populate the surface of the lens, we performed immunolabeling for CD68 and GR1 on cryosections of normal eyes (Figures 8A,C and 9A,B) and at 1 day after corneal debridement wounding (Figures 8B,D and 9C-H). Each section was imaged by confocal microscopy in two areas: the surface of the lens equatorial zone (Figures 8A,B and 9A,C,E,F), and the lens anterior surface (Figures 8C,D and 9B,D,G,H). In normal eyes, CD68+ cells were never seen migrating along the lens capsule in the equatorial or anterior regions of the surface of the lens (Figure 8A,C). The equatorial and anterior surfaces of the lens were also devoid of GR1+ cells in normal eyes (Figure 9A,B). When the surveillance of the lens by immune cells is activated in response to corneal wounding, both CD68+ (Figure 8B,D) and GR1+ (Figure 9C-H) immune cells populate the lens equatorial and anterior surfaces. In addition, a subpopulation of these GR1 cells were observed migrating through the perlecan-rich capsule in the anterior epithelium region, shown in 3D structural images created from confocal Z-stacks (Figure 8G,H, arrowheads). This finding shows that these immune cells, activated to surveil the lens in response to a corneal wounding, can cross into the lens itself as part of their response to ocular injury.

### 3.6 | SEM imaging of immune cells that associate with ciliary zonules on the surface of the lens in response to cornea wounding

Imaging of whole adult mouse lenses that had been removed from the eye and labeled for both MAGP1 and F-actin shows the MAGP1-rich ciliary zonules extending along the lens surface (Figure 10A,D,F, arrows) and entering the lens, becoming inserted within the lens epithelium which is labeled for F-actin (Figure 10A-F, arrowheads). We also examined lens cell surface-associated zonules by performing scanning electron microscopy (SEM) imaging studies of the lens surface in unwounded eyes (Figure 11). Lenses removed from normal eyes were found to have extensive ciliary zonules that extend and spread out in thinner and thinner fibrils in an anterior direction along the lens surface (Figure 11A-D, shown from low to high magnification). These fibrils were acellular (Figure 11B-D). In contrast, as a response to cornea wounding (Figure 12), groups of immune cells were often in association with the lens-surface linked zonule fibrils (Figure 12B-I). These cells were of various phenotypes, some with morphologies typical of motile immune cells (Figure 12B-E), others more rounded and embedded within the zonule-like fibrils extended along the surface of the lens (Figure 12F-I), similar in appearance to neutrophil extracellular traps (NETs).<sup>56,57</sup>

## 4 | DISCUSSION

The eye is among the few sites in the body where barriers to vascularization are essential to maintain function. After birth, the vasculature of the eye is restricted to areas outside the central light path. In the cornea, the limbal region is the



principle source of immune cells following injury.<sup>53,54</sup> For the avascular lens, suspended in the center of the eye on the fibrillin and MAGP1-rich zonules that link it to the ciliary body, the absence of a vasculature presents a challenge for an immune response to injury or dysgenesis and has led to the assumption that immune cells have no path or access to

the lens. Previous studies from our lab of the dysgenic lenses of adult N-cad<sup>Δlens</sup> mice revealed that immune cells enter these lenses to populate the damaged areas of this tissue,<sup>1</sup> and suggested the potential path to the lens for these immune cells was the ciliary zonules. We now provide evidence that immune cells known to be present in vasculature-rich uveal

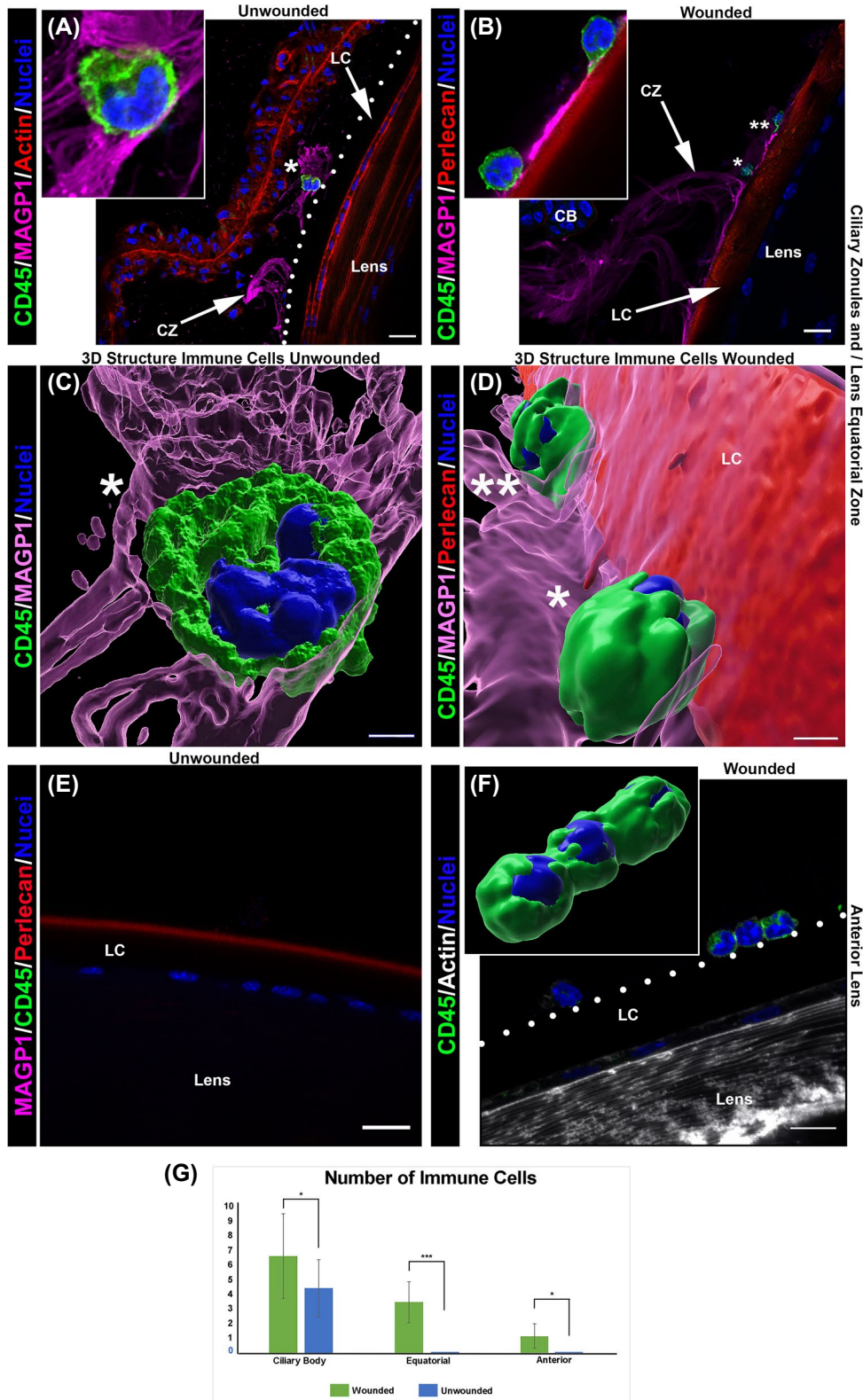


**FIGURE 7** Surveillance of the lens by immune cells is induced in response to corneal debridement wounding. A-D, Whole mouse eye cryosections imaged between the ciliary body and the lens and along the anterior surface of the lens (E,F) in (A,C,E) unwounded eyes and (B,D,F) at 1 day post-corneal debridement wounding. A, Co-immunolabeling for MAGP1 (purple) and CD45 (green), also labeled for actin (red) and nuclei (blue). B,D, and E, Co-immunolabeling for MAGP1 (purple), CD45 (green), and perlecan (red), also labeled for nuclei (blue). C, Co-immunolabeling for MAGP1 (purple), CD45 (green), and nuclei (blue). F, Immunolabeled for CD45 (green) and co-labeled for actin (white) and nuclei (blue). Insets in A,B are high magnification views of the immune cells. (C,D, inset of F) 3D structural images created from confocal Z-stacks. Asterisks indicate the same cells in different images. Dotted line indicates the surface of the lens. G, Quantification of the number of CD45+ immune cells present in three areas: the ciliary body, the equatorial region and the anterior epithelium in wounded and unwounded eyes. Graph demonstrates mean  $\pm$  SD, data analyzed by *t* test with \**P* < .05; \*\*\**P* < .001. In unwounded eyes immune cells are found traveling on ciliary zonules between the ciliary body and the lens but were not associated with zonule fibrils that extend along the surface of the lens. In contrast, at 1D post-corneal debridement wounding, surveillance of the lens by immune cells is induced and CD45+ cells are found traveling along the zonule fibers that extend along the surface of the lens and more anterior regions of the lens surface. Studies are representative of at least three independent experiments. Magnification bars = 20  $\mu$ m A,B,E; = 3  $\mu$ m C,D; = 10  $\mu$ m F. CB, ciliary body; CZ, ciliary zonules; LC, lens capsule

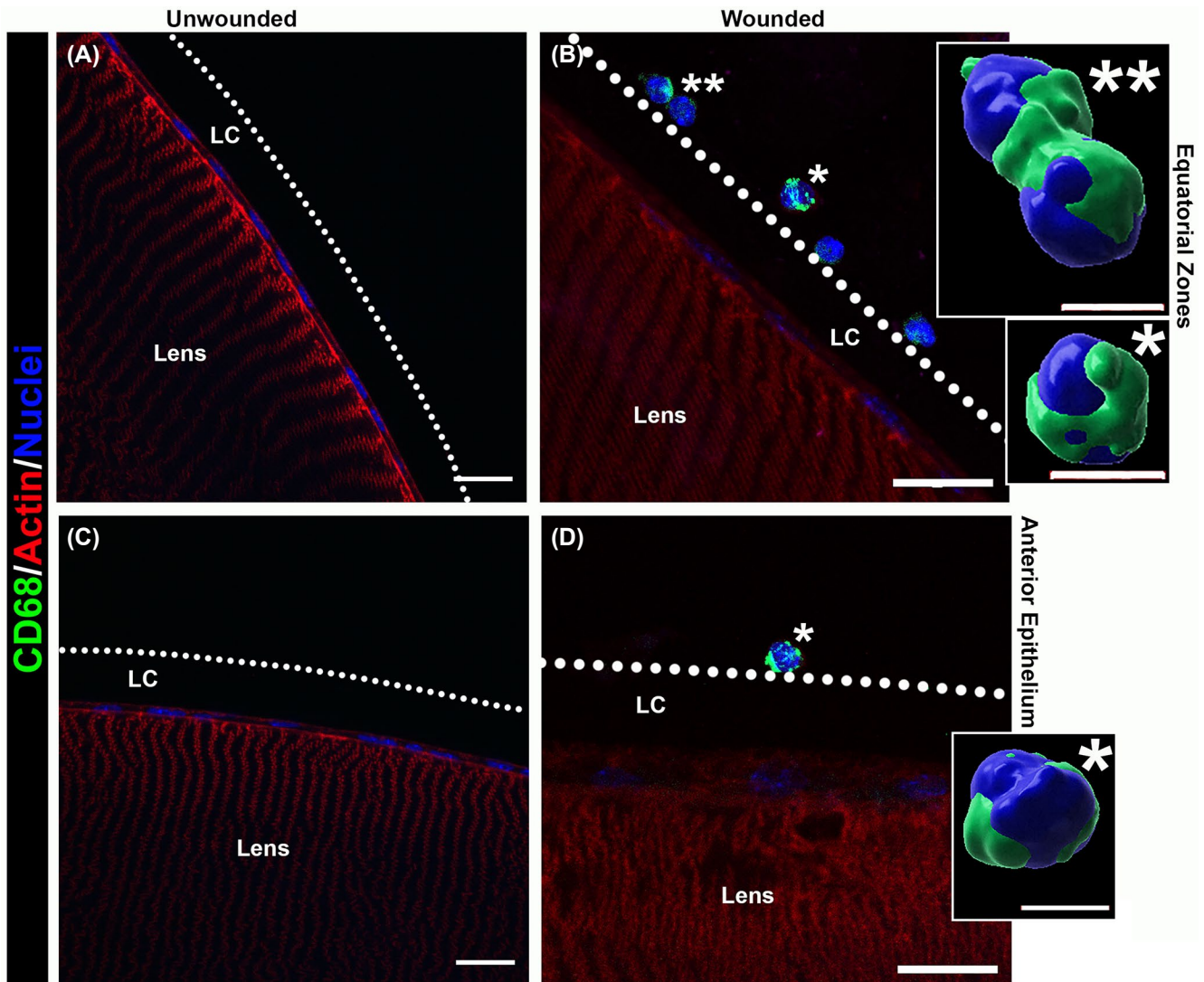


**FIGURE 8** Surveillance of the lens by immune cells in response to corneal debridement wounding involves macrophages. Whole mouse eye cryosections of (A,C) unwounded eyes and (B,D) at 1 day post-corneal debridement wounding. A-D, Immunolabeled for CD68 (green) and co-labeled for actin (red) and nuclei (blue). Asterisks indicate the same cells in different images. Dotted line indicates the surface of the lens. Insets in B and D are 3D structural images created from confocal Z-stacks. In unwounded eyes CD68+ cells are found traveling along the zonules between the ciliary body and the lens but not along the lens surface. In response to corneal wounding both CD68+ are induced to migrate along the lens capsule toward the anterior of the lens. Studies are representative of at least three independent experiments. Magnification bars = 20  $\mu$ m A-D; = 3  $\mu$ m for insets. LC, lens capsule. (A,C,D) Single optical plane; (B) projection image

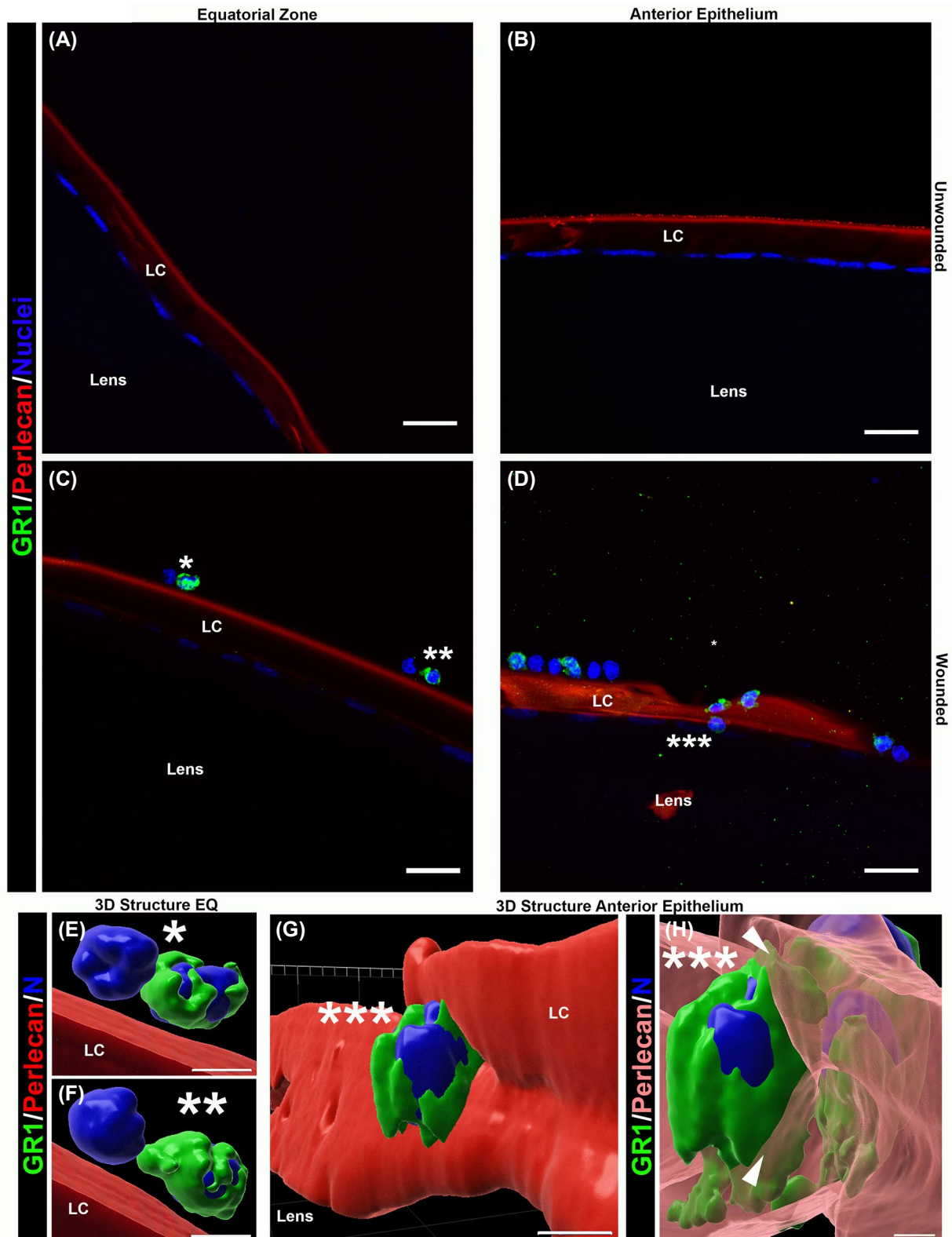


**FIGURE 9** Surveillance of the lens in response to corneal debridement wounding involves leukocytes. Whole mouse eye cryosections of (A,B) unwounded eyes and (C-H) at 1 day post-corneal debridement wounding. A-H, Co-immunolabeled for GR1 (green) and perlecan (A-G red, H, pink), co-labeled for nuclei (blue). A,C,E,F, Imaged along the equatorial zone; B,D,G,H, imaged along the anterior epithelium. E-H, are 3D structural images created from confocal Z-stacks. Asterisks indicate the same cells in different images. In response to corneal wounding GR1+ cells are induced to migrate along the lens capsule toward the anterior of the lens and in the anterior of the lens the GR1+ cells transit the lens capsule. Studies are representative of at least three independent experiments. Magnification bars = 20  $\mu$ m A-D; =5  $\mu$ m E-G; =2  $\mu$ m H. LC, lens capsule. (A-C) Single optical plane; (D) projection image



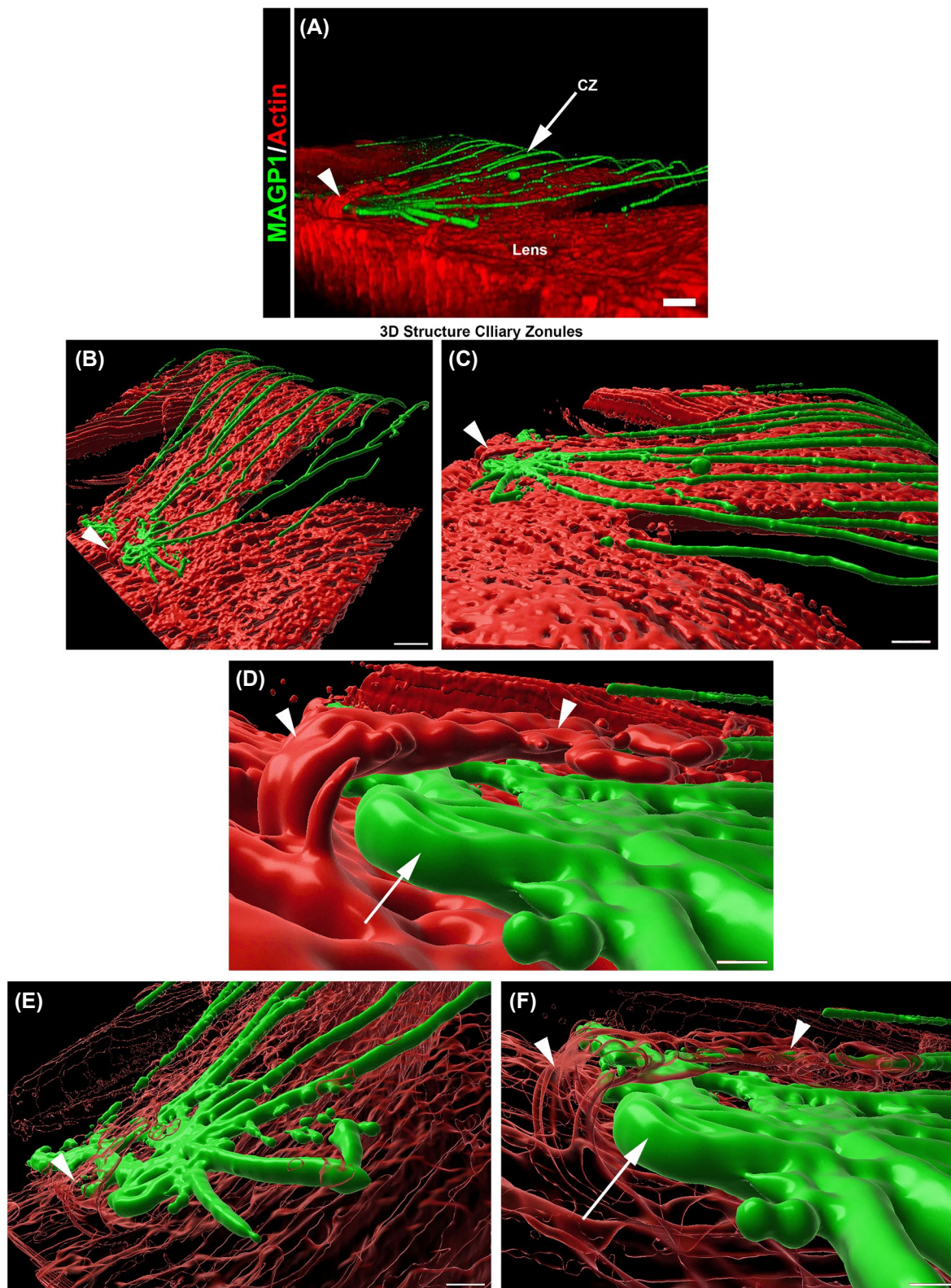


**FIGURE 10** Association of MAGP1-rich ciliary zonules with the lens. A-F, Imaging of whole lenses isolated from uninjured mouse eyes immunolabeled for MAGP1 (green) and co-labeled for actin (red). (A) is a 3D image created using Velocity software, (B-F) are 3D structural images created from confocal Z-stacks using Imaris software. The images show zonule fibers associated with the lens surface and inserting into the lens epithelium. Arrows denote ciliary zonules, arrowheads denote F-actin labeling of lens cells. Studies are representative of at least three independent experiments. Magnification bars = 20  $\mu\text{m}$  A,C; =30  $\mu\text{m}$  B; =10  $\mu\text{m}$  D,F, =15  $\mu\text{m}$  E. CZ = ciliary zonules



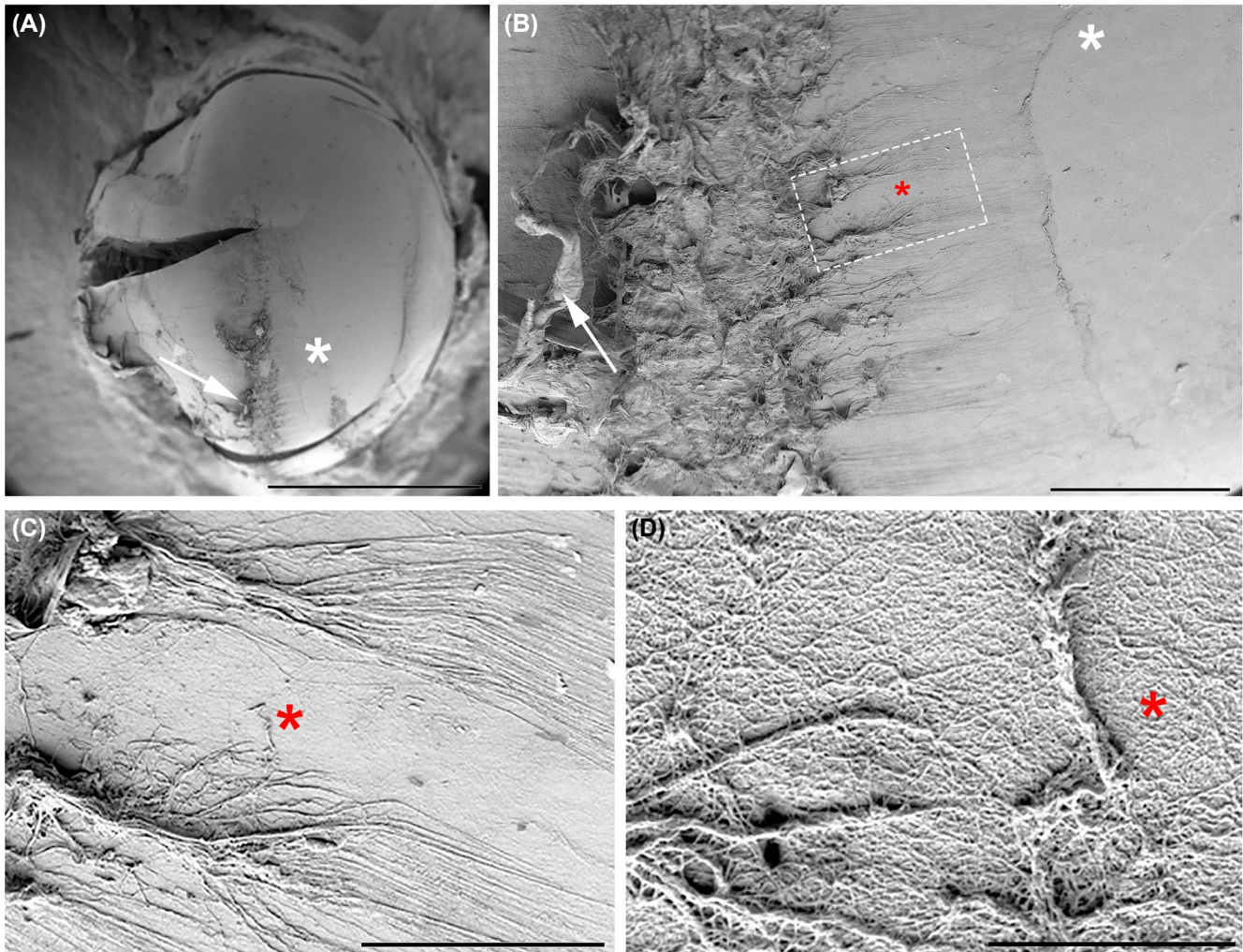


**FIGURE 11** Ciliary zonules extended along the surface of the normal lens. SEM images of the surface of the mouse lens from unwounded eyes. Asterisks (A-D) denote regions just anterior to the lens equatorial zone represented at increasingly higher magnifications. Ciliary zonules are seen to extend from the lens equator along the anterior surface of the lens in the normal eye. Cells are rarely detected in the zonule fibers that extend along the surface of the lens in unwounded eyes. Studies are representative of three independent lenses from control mice. Magnification bars = 1 mm A; =100  $\mu$ m B; =30  $\mu$ m C, =3  $\mu$ m D

tissues, including the ciliary body and iris,<sup>8,9,11</sup> travel along the ciliary zonule fibrils that are extended along the surface of the lens and provide for surveillance of the lens by immune cells in response to debridement injury to the cornea (Figure 13).

Prior to corneal wounding, immune cells populate the ciliary zonules between the ciliary body and the lens equator. In the unwounded eye, these immune cells did not associate with the anterior- or posterior-directed ciliary zonules that extend along the surface of the lens. The results of this study now show, for the first time, that immune cells are associated with the ciliary zonules that extend from the equatorial to the anterior surface of the lens in response to a debridement wound of the cornea, and suggest they are sourced from the vasculature-rich ciliary zonules. Immune cells, including monocytes, macrophages, and neutrophils migrate along these lens-associated zonule fibers during the first day

following cornea wounding, and come to locate to the lens anterior surface just beyond the extent of the zonule fibers, likely associated with the matrix components of the anterior lens (Figure 13).

Our studies now show that the ECM protein MAGP1, a principal molecular component of the ciliary zonules is upregulated in the central cornea following debridement wounding. In our previous RNAseq study, data mining analysis shows that MAGP1 (MFAP2) RNA is not expressed by the cells of the corneal epithelium in either unwounded or wounded corneas, but is expressed by stromal cells, increasing 1.4-fold following wounding,<sup>58</sup> a result consistent with the protein data shown here. MAGP1 binds to and activates latent and active forms of TGF $\beta$ ,<sup>30,34,59</sup> which is known to increase in the aqueous humor in the setting of anterior chamber inflammation, such as experimental autoimmune uveoretinitis, as well as glaucoma.<sup>60,61</sup> MAGP1



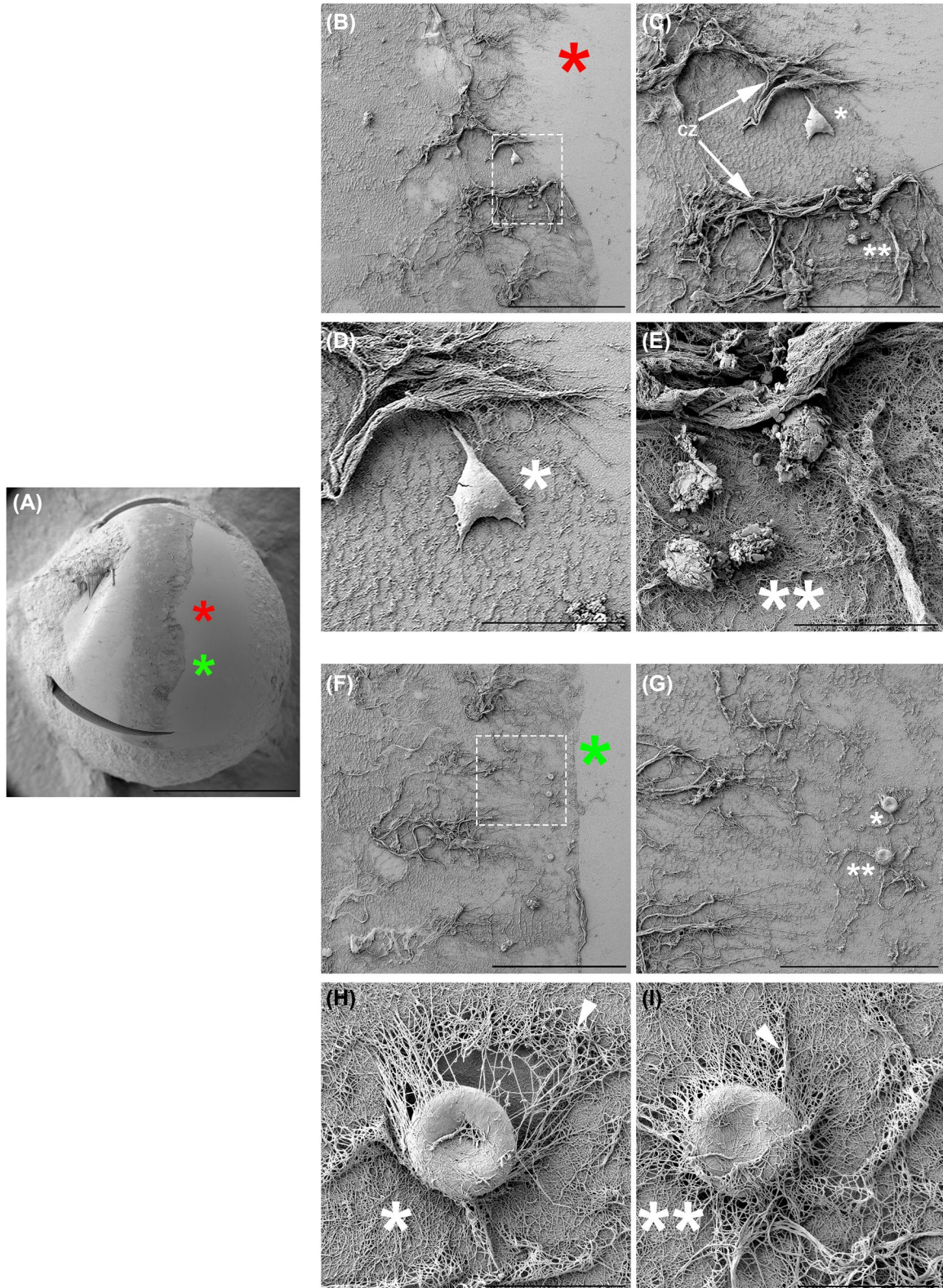


**FIGURE 12** Cells populate zonule fibers that extend along the surface of the lens in response to cornea wounding. SEM images of the surface of the mouse lens at 1D post-corneal wounding. Asterisks denote regions just anterior to the lens equatorial zone represented at increasingly higher magnifications. Cells with rounded morphologies typical of immune cells as well as cells with migratory phenotypes are prevalent, and often intertwined with the anterior extending zonules, after wounding. Studies are representative of three independent lenses from corneal wounded mice. Magnification bars = 1 mm A; = 100  $\mu$ m B,F; = 50  $\mu$ m C, = 10  $\mu$ m D,E; = 40  $\mu$ m G; = 5  $\mu$ m H,I



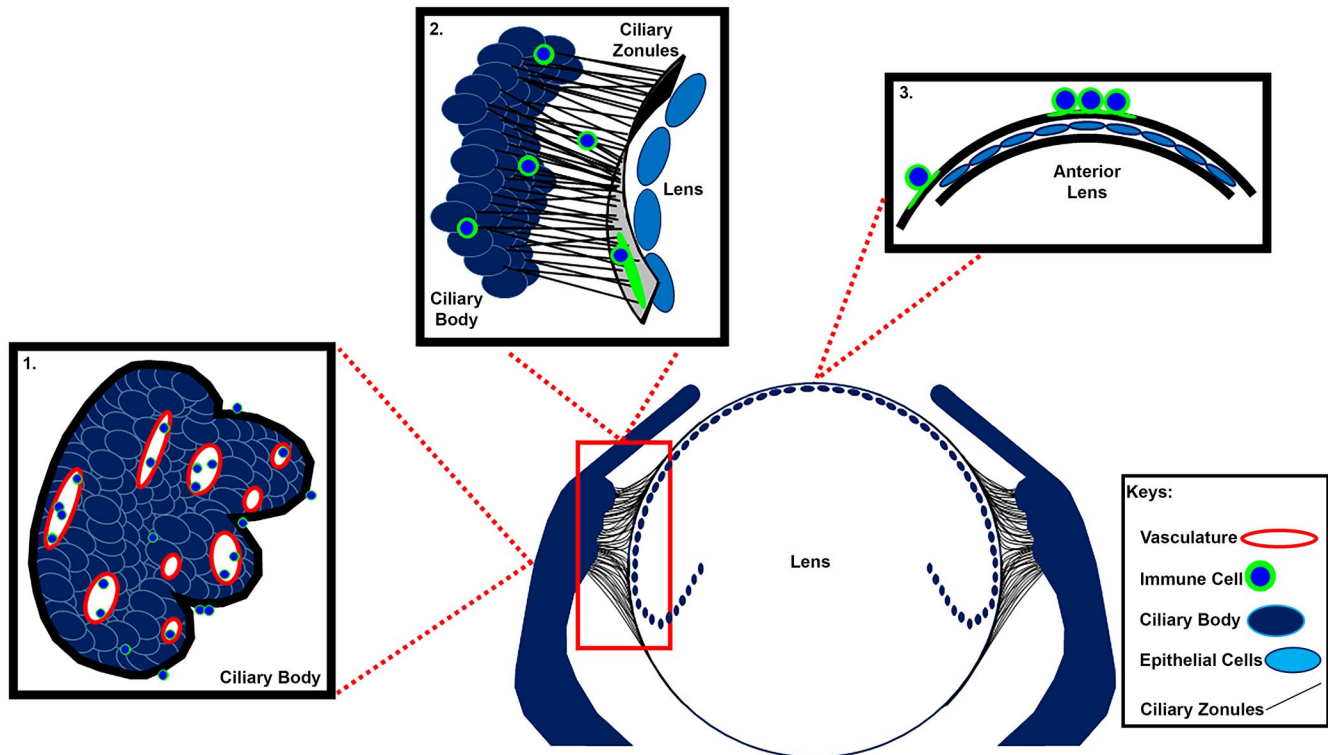


**FIGURE 13** Model depicting the immune response to the along the lens-associated ciliary zonules following corneal debridement wounding. 1. Ciliary body. 2. Ciliary body, ciliary zonules, and the lens equator. 3. Lens anterior surface. Within 1 day following corneal debridement wounding, immune cells increase in the ciliary body, and come to populate the ciliary zonules along the equatorial surface of the lens and are also found along the anterior surface of the lens, where we find them transiting the lens capsule

could be actively involved in the movement of immune cells to the lens along the lens-associated ciliary zonules, as well as in the wounded cornea. Both HA and TSP-1, which associate directly or indirectly with fibrillin,<sup>62,63</sup> are also likely factors in the process that promotes immune cell migration across the ciliary zonules to surveil the avascular lens. HA is known to promote inflammation in response to wound healing<sup>64</sup> and TSP-1 to mediate cell matrix interactions.<sup>35</sup> TSP-1 was found to be associated with both the ciliary zonule microfibrils and the superficial surface of the anterior lens capsule.

It is also important to consider this immune response in the context of an adaptive immune response. It has been shown that antigens from the avascular cornea are able to travel to the secondary lymphatic tissue including the cervical and submandibular draining lymph node and spleen via antigen-presenting dendritic cells and macrophages.<sup>12,65,66</sup> If these antigens are delivered in the context of innate-immune cell activation, this can also result in antigen-specific T-cell activation and response, which may in turn contribute to further surveillance of the cornea and lens.

SEM studies show that many of the immune cells that associate with the lens surface in response to cornea wounding are integrated into the zonule fiber meshwork, including ones with rounded morphologies or flattened morphologies

characteristic of migratory phenotypes. Migratory immune cells, especially migratory dendritic cells, are critical for both protective pro-inflammatory and anti-inflammatory responses.<sup>67</sup> SEM studies also demonstrate that the ciliary zonule-associated immune cells are similar in appearance to NETs.<sup>56</sup> NETs have previously been primarily linked to a role in antimicrobial and antiviral defense, to prevent infectious spread, including in the eye.<sup>68,69</sup> NETs have also been linked to both pro- and anti-inflammatory functions<sup>70-74</sup> and recent eye studies also suggest a role for NETs in eye immunomodulation.<sup>75</sup>

Our findings also demonstrate the migration of immune cells through the lens capsule. In our previous studies of dysgenic lenses,<sup>1</sup> we showed the presence of immune cells within the lens in spite of an intact lens capsule. Here, we show for the first time, immune invasion across the lens capsule in the absence of lens pathology. This highlights a potential role for immune cells in cataract formation, especially in the setting of pro-inflammatory conditions which have been linked to increased and complicated cataract formation in the past, such as pediatric uveitis,<sup>76-78</sup> viral anterior uveitis,<sup>79-81</sup> and intermediate uveitis.<sup>82-84</sup> Additionally, our discovery is consistent with the finding that an innate immune response is active post-cataract surgery within the lens, as seen in Posterior Capsule Opacification (PCO) studies,<sup>85</sup> which also

demonstrated an induction of S100A9 in the post-cataract surgery setting. The S100 proteins, known to be damage-associated molecular patterns (DAMPs) also known as alarmins, are capable of activating immune cell recruitment for tissue repair.<sup>86</sup> In light of this, our understanding of multiple ocular diseases likely depends on our furthered understanding of ocular immune regulation.

Much progress has been made over the years in understanding immune privilege in the eye since the term was first introduced.<sup>87</sup> The innovative adaptations for immune cells to be recruited to immune protected sites in the eye indicate that, like the brain, the lens is better described as immune quiescent.<sup>88</sup> Our findings here show that in the adult eye there is an active mechanism for immune cells to surveille the lens. In response to a corneal injury, immune cells that are normally associated with zonules between the ciliary body and the lens are signaled to accumulate along the zonules that extend along the surface of the lens and further migrate along the anterior aspect of the lens, with some even traversing the lens capsule. Going forward, it is clear that it now becomes important to define the mechanisms governing the role of fibrillin, MAGP1 and their associated molecules in promoting immune cell migration along lens zonule fibers.

## ACKNOWLEDGMENTS

We thank Robert Mecham for providing us with his MAGP1 antibody for our studies. This work was funded by the National Institute of Health grant EY021784 to ASM and MAS.

## CONFLICT OF INTEREST

There is no conflict of interest.

## AUTHOR CONTRIBUTIONS

J. DeDreu conducted experiments and created the figures for the paper, C.J. Bowen, S. Pal-Ghosh, and P. Parlanti conducted experiments for the paper, C.M. Logan conducted experiments for the paper and assisted in writing the manuscript, M.A. Stepp conceived ideas for the project, designed and analyzed studies, and contributed to writing of the manuscript, A.S. Menko conceived the idea for the project, designed, coordinated and analyzed the studies, and wrote the paper. All authors approved the final manuscript.

## REFERENCES

- Logan CM, Bowen CJ, Menko AS. Induction of immune surveillance of the dysmorphic lens. *Sci Rep*. 2017;7:16235.
- Logan CM, Rajakaruna S, Bowen C, Radice GL, Robinson ML, Menko AS. N-cadherin regulates signaling mechanisms required for lens fiber cell elongation and lens morphogenesis. *Dev Biol*. 2017;428:118-134.
- McLeod DS, Hasegawa T, Baba T, et al. From blood islands to blood vessels: morphologic observations and expression of key molecules during hyaloid vascular system development. *Invest Ophthalmol Vis Sci*. 2012;53:7912-7927.
- Hegde S, Srivastava O. Different gene knockout/transgenic mouse models manifesting persistent fetal vasculature: are integrins to blame for this pathological condition? *Life Sci*. 2017;171:30-38.
- Nishitani K, Sasaki K. Macrophage localization in the developing lens primordium of the mouse embryo - an immunohistochemical study. *Exp Eye Res*. 2006;83:223-228.
- Zhu M, Madigan MC, van Driel D, et al. The human hyaloid system: cell death and vascular regression. *Exp Eye Res*. 2000;70:767-776.
- Ito M, Yoshioka M. Regression of the hyaloid vessels and pupillary membrane of the mouse. *Anat Embryol*. 1999;200:403-411.
- McMenamin PG, Holthouse I, Holt PG. Class II major histocompatibility complex (Ia) antigen-bearing dendritic cells within the iris and ciliary body of the rat eye: distribution, phenotype and relation to retinal microglia. *Immunology*. 1992;77:385-393.
- Forrester JV, Xu H, Lambe T, Cornall R. Immune privilege or privileged immunity? *Mucosal Immunol*. 2008;1:372-381.
- Ginhoux F, Greter M, Leboeuf M, et al. Fate mapping analysis reveals that adult microglia derive from primitive macrophages. *Science*. 2010;330:841-845.
- Forrester JV, Xu H. Good news-bad news: the Yin and Yang of immune privilege in the eye. *Front Immunol*. 2012;3:338.
- Plskova J, Duncan L, Holan V, Filipic M, Kraal G, Forrester JV. The immune response to corneal allograft requires a site-specific draining lymph node. *Transplantation*. 2002;73:210-215.
- Plskova J, Kuffova L, Holan V, Filipic M, Forrester JV. Evaluation of corneal graft rejection in a mouse model. *Br J Ophthalmol*. 2002;86:108-113.
- Kuffova L, Netukova M, Duncan L, Porter A, Stockinger B, Forrester JV. Cross presentation of antigen on MHC class II via the draining lymph node after corneal transplantation in mice. *J Immunol*. 2008;180:1353-1361.
- Chen L, Cursiefen C, Barabino S, Zhang Q, Dana MR. Novel expression and characterization of lymphatic vessel endothelial hyaluronate receptor 1 (LYVE-1) by conjunctival cells. *Invest Ophthalmol Vis Sci*. 2005;46:4536-4540.
- Cursiefen C, Chen L, Borges LP, et al. VEGF-A stimulates lymphangiogenesis and hemangiogenesis in inflammatory neovascularization via macrophage recruitment. *J Clin Invest*. 2004;113:1040-1050.
- Xu H, Chen M, Reid DM, Forrester JV. LYVE-1-positive macrophages are present in normal murine eyes. *Invest Ophthalmol Vis Sci*. 2007;48:2162-2171.
- Xu H, Sta Iglesia DD, Kielczewski JL, et al. Characteristics of progenitor cells derived from adult ciliary body in mouse, rat, and human eyes. *Invest Ophthalmol Vis Sci*. 2007;48:1674-1682.
- Taylor AW, Alard P, Yee DG, Streilein JW. Aqueous humor induces transforming growth factor-beta (TGF-beta)-producing regulatory T-cells. *Curr Eye Res*. 1997;16:900-908.
- Nishida T, Taylor AW. Specific aqueous humor factors induce activation of regulatory T cells. *Invest Ophthalmol Vis Sci*. 1999;40:2268-2274.
- Denniston AK, Tomlins P, Williams GP, et al. Aqueous humor suppression of dendritic cell function helps maintain immune regulation in the eye during human uveitis. *Invest Ophthalmol Vis Sci*. 2012;53:888-896.
- Denniston AK, Kottoor SH, Khan I, et al. Endogenous cortisol and TGF-beta in human aqueous humor contribute to ocular

- immune privilege by regulating dendritic cell function. *J Immunol.* 2011;186:305-311.
23. Joachim SC, Bruns K, Lackner KJ, Pfeiffer N, Grus FH. Antibodies to alpha B-crystallin, vimentin, and heat shock protein 70 in aqueous humor of patients with normal tension glaucoma and IgG antibody patterns against retinal antigen in aqueous humor. *Curr Eye Res.* 2007;32:501-509.
  24. Bell K, Und Hohenstein-Blaul NVT, Teister J, Grus F. Modulation of the immune system for the treatment of glaucoma. *Curr Neuropharmacol.* 2018;16:942-958.
  25. Shi Y, Tu Y, De Maria A, Mecham RP, Bassnett S. Development, composition, and structural arrangements of the ciliary zonule of the mouse. *Invest Ophthalmol Vis Sci.* 2013;54:2504-2515.
  26. Beene LC, Wang LW, Hubmacher D, et al. Nonselective assembly of fibrillin 1 and fibrillin 2 in the rodent ocular zonule and in cultured cells: implications for Marfan syndrome. *Invest Ophthalmol Vis Sci.* 2013;54:8337-8344.
  27. Hubmacher D, Reinhardt DP, Plessec T, Schenke-Layland K, Apte SS. Human eye development is characterized by coordinated expression of fibrillin isoforms. *Invest Ophthalmol Vis Sci.* 2014;55:7934-7944.
  28. Hanssen E, Franc S, Garrone R. Synthesis and structural organization of zonular fibers during development and aging. *Matrix Biol.* 2001;20:77-85.
  29. De Maria A, Wilmarth PA, David LL, Bassnett S. Proteomic analysis of the bovine and human ciliary zonule. *Invest Ophthalmol Vis Sci.* 2017;58:573-585.
  30. Mecham RP, Gibson MA. The microfibril-associated glycoproteins (MAGPs) and the microfibrillar niche. *Matrix Biol.* 2015;47:13-33.
  31. Zuliani-Alvarez L, Marzeda AM, Deligne C, et al. Mapping tenascin-C interaction with toll-like receptor 4 reveals a new subset of endogenous inflammatory triggers. *Nat Commun.* 2017;8:1595.
  32. Marzeda AM, Midwood KS. Internal affairs: tenascin-C as a clinically relevant, endogenous driver of innate immunity. *J Histochem Cytochem.* 2018;66:289-304.
  33. Halper J, Kjaer M. Basic components of connective tissues and extracellular matrix: elastin, fibrillin, fibulins, fibrinogen, fibronectin, laminin, tenascins and thrombospondins. *Adv Exp Med Biol.* 2014;802:31-47.
  34. Travis MA, Sheppard D. TGF-beta activation and function in immunity. *Annu Rev Immunol.* 2014;32:51-82.
  35. Calzada MJ, Annis DS, Zeng B, et al. Identification of novel beta1 integrin binding sites in the type 1 and type 2 repeats of thrombospondin-1. *J Biol Chem.* 2004;279:41734-41743.
  36. Forslow A, Liu Z, Sundqvist KG. Receptor communication within the lymphocyte plasma membrane: a role for the thrombospondin family of matricellular proteins. *Cellular Mol Life Sci.* 2007;64:66-76.
  37. Jackson DG, Prevo R, Clasper S, Banerji S. LYVE-1, the lymphatic system and tumor lymphangiogenesis. *Trends Immunol.* 2001;22:317-321.
  38. Jackson DG. The lymphatics revisited: new perspectives from the hyaluronan receptor LYVE-1. *Trends Cardiovasc Med.* 2003;13:1-7.
  39. Jackson DG. Biology of the lymphatic marker LYVE-1 and applications in research into lymphatic trafficking and lymphangiogenesis. *APMIS.* 2004;112:526-538.
  40. Dollt C, Becker K, Michel J, et al. The shedded ectodomain of Lyve-1 expressed on M2-like tumor-associated macrophages inhibits melanoma cell proliferation. *Oncotarget.* 2017;8:103682-103692.
  41. Nishida-Fukuda H, Araki R, Shudou M, et al. Ectodomain shedding of lymphatic vessel endothelial hyaluronan receptor 1 (LYVE-1) is induced by vascular endothelial growth factor A (VEGF-A). *J Biol Chem.* 2016;291:10490-10500.
  42. Pajoohesh-Ganji A, Pal-Ghosh S, Tadvalkar G, Stepp MA. K14 + compound niches are present on the mouse cornea early after birth and expand after debridement wounds. *Dev Dynam.* 2016;245:132-143.
  43. Meek KM, Knupp C. Corneal structure and transparency. *Prog Retin Eye Res.* 2015;49:1-16.
  44. White TL, Lewis P, Hayes S, et al. The structural role of elastic fibers in the cornea investigated using a mouse model for marfan syndrome. *Invest Ophthalmol Vis Sci.* 2017;58:2106-2116.
  45. Feneck EM, Lewis PN, Ralphs J, Meek KM. A comparative study of the elastic fibre system within the mouse and human cornea. *Exp Eye Res.* 2018;177:35-44.
  46. Blanco-Mezquita JT, Hutcheon AE, Zieske JD. Role of thrombospondin-1 in repair of penetrating corneal wounds. *Invest Ophthalmol Vis Sci.* 2013;54:6262-6268.
  47. Matsuba M, Hutcheon AE, Zieske JD. Localization of thrombospondin-1 and myofibroblasts during corneal wound repair. *Exp Eye Res.* 2011;93:534-540.
  48. Knop E, Knop N. Anatomy and immunology of the ocular surface. *Chem Immunol Allergy.* 2007;92:36-49.
  49. Lemp MA. Dry eye (Keratoconjunctivitis Sicca), rheumatoid arthritis, and Sjogren's syndrome. *Am J Ophthalmol.* 2005;140:898-899.
  50. Lee YC, Chang HH, Liu CH, et al. Methyl palmitate: a potent vasodilator released in the retina. *Invest Ophthalmol Vis Sci.* 2010;51:4746-4753.
  51. Hamrah P, Zhang Q, Liu Y, Dana MR. Novel characterization of MHC class II-negative population of resident corneal Langerhans cell-type dendritic cells. *Invest Ophthalmol Vis Sci.* 2002;43:639-646.
  52. Pal-Ghosh S, Pajoohesh-Ganji A, Menko AS, et al. Cytokine deposition alters leukocyte morphology and initial recruitment of monocytes and gammadeltaT cells after corneal injury. *Invest Ophthalmol Vis Sci.* 2014;55:2757-2765.
  53. Mobaraki M, Abbasi R, Omidian Vandchali S, Ghaffari M, Moztafzadeh F, Mozafari M. Corneal repair and regeneration: current concepts and future directions. *Front Bioeng Biotechnol.* 2019;7:135.
  54. Gonzalez G, Sasamoto Y, Ksander BR, Frank MH, Frank NY. Limbal stem cells: identity, developmental origin, and therapeutic potential. *Wiley Interdiscip Rev Dev Biol.* 2018;7(2):e303.
  55. Bassnett S. A method for preserving and visualizing the three-dimensional structure of the mouse zonule. *Exp Eye Res.* 2019;185:107685.
  56. Krautgartner WD, Klappacher M, Hannig M, et al. Fibrin mimics neutrophil extracellular traps in SEM. *Ultrastruct Pathol.* 2010;34:226-231.
  57. Papayannopoulos V. Neutrophil extracellular traps in immunity and disease. *Nat Rev Immunol.* 2018;18:134-147.
  58. Stepp MA, Pal-Ghosh S, Tadvalkar G, Li L, Brooks SR, Morasso MI. Molecular basis of Mitomycin C enhanced corneal sensory nerve repair after debridement wounding. *Sci Rep.* 2018;8:16960.
  59. Craft CS, Pietka TA, Schappe T, et al. The extracellular matrix protein MAGP1 supports thermogenesis and protects against



- obesity and diabetes through regulation of TGF- $\beta$ . *Diabetes*. 2014;63:1920-1932.
60. Ohta K, Wiggert B, Yamagami S, Taylor AW, Streilein JW. Analysis of immunomodulatory activities of aqueous humor from eyes of mice with experimental autoimmune uveitis. *J Immunol*. 2000;164:1185-1192.
  61. Agarwal P, Daher AM, Agarwal R. Aqueous humor TGF- $\beta$ 2 levels in patients with open-angle glaucoma: a meta-analysis. *Mol Vis*. 2015;21:612-620.
  62. Chan FL, Choi HL, Underhill CB. Hyaluronan and chondroitin sulfate proteoglycans are colocalized to the ciliary zonule of the rat eye: a histochemical and immunocytochemical study. *Histochem Cell Biol*. 1997;107:289-301.
  63. Kuznetsova SA, Issa P, Perruccio EM, et al. Versican-thrombospondin-1 binding in vitro and colocalization in microfibrils induced by inflammation on vascular smooth muscle cells. *J Cell Sci*. 2006;119:4499-4509.
  64. Litwiniuk M, Krejner A, Speyrer MS, Gauto AR, Grzela T. Hyaluronic acid in inflammation and tissue regeneration. *Wounds*. 2016;28:78-88.
  65. Camelo S, Kezic J, Shanley A, Rigby P, McMenamin PG. Antigen from the anterior chamber of the eye travels in a soluble form to secondary lymphoid organs via lymphatic and vascular routes. *Invest Ophthalmol Vis Sci*. 2006;47:1039-1046.
  66. Dang Z, Kuffova L, Liu L, Forrester JV. Soluble antigen traffics rapidly and selectively from the corneal surface to the eye draining lymph node and activates T cells when codelivered with CpG oligonucleotides. *J Leukoc Biol*. 2014;95:431-440.
  67. Worbs T, Hammerschmidt SI, Forster R. Dendritic cell migration in health and disease. *Nat Rev Immunol*. 2017;17:30-48.
  68. Kruger P, Saffarzadeh M, Weber AN, et al. Neutrophils: between host defence, immune modulation, and tissue injury. *PLoS Pathog*. 2015;11:e1004651.
  69. Thanabalasuriar A, Scott BNV, Peiseler M, et al. Neutrophil extracellular traps confine *Pseudomonas aeruginosa* ocular biofilms and restrict brain invasion. *Cell Host Microbe*. 2019;25:526-536.e524.
  70. Thanabalasuriar A, Kubes P. Rise and shine: open your eyes to produce anti-inflammatory NETs. *J Leukoc Biol*. 2019;105:1083-1084.
  71. Schauer C, Janko C, Munoz LE, et al. Aggregated neutrophil extracellular traps limit inflammation by degrading cytokines and chemokines. *Nat Med*. 2014;20:511-517.
  72. Li RHL, Tablin F. A comparative review of neutrophil extracellular traps in sepsis. *Front Vet Sci*. 2018;5:291.
  73. Hakkim A, Furnrohr BG, Amann K, et al. Impairment of neutrophil extracellular trap degradation is associated with lupus nephritis. *Proc Natl Acad Sci USA*. 2010;107:9813-9818.
  74. Mahajan A, Herrmann M, Munoz LE. Clearance deficiency and cell death pathways: a model for the pathogenesis of SLE. *Front Immunol*. 2016;7:35.
  75. Mahajan A, Gruneboom A, Petru L, et al. Frontline Science: aggregated neutrophil extracellular traps prevent inflammation on the neutrophil-rich ocular surface. *J Leukoc Biol*. 2019;105:1087-1098.
  76. Blum-Hareuveni T, Seguin-Greenstein S, Kramer M, et al. Risk factors for the development of cataract in children with uveitis. *Am J Ophthalmol*. 2017;177:139-143.
  77. Ferrara M, Eggenschwiler L, Stephenson A, et al. The challenge of pediatric uveitis: tertiary referral center experience in the United States. *Ocul Immunol Inflamm*. 2019;27:410-417.
  78. Chan NS, Choi J, Cheung CMG. Pediatric Uveitis. *Asia Pac J Ophthalmol*. 2018;7:192-199.
  79. Chee SP, Bacsal K, Jap A, Se-Thoe SY, Cheng CL, Tan BH. Clinical features of cytomegalovirus anterior uveitis in immunocompetent patients. *Am J Ophthalmol*. 2008;145:834-840.
  80. Bouchenaki N, Herbot CP. Fluorescein angiographic findings and clinical features in Fuchs' uveitis. *Int Ophthalmol*. 2010;30:511-519.
  81. Al-Mansour YS, Al-Rajhi AA, Al-Dhibi H, Abu El-Asrar AM. Clinical features and prognostic factors in Fuchs' uveitis. *Int Ophthalmol*. 2010;30:501-509.
  82. Meier FM, Tuft SJ, Pavesio CE. Cataract surgery in uveitis. *Ophthalmol Clin North Am*. 2002;15:365-373.
  83. Bonfioli AA, Damico FM, Curi AL, Orefice F. Intermediate uveitis. *Semin Ophthalmol*. 2005;20:147-154.
  84. Dick AD, Tundia N, Sorg R, et al. Risk of ocular complications in patients with noninfectious intermediate uveitis, posterior uveitis, or panuveitis. *Ophthalmology*. 2016;123:655-662.
  85. Jiang J, Shihan MH, Wang Y, Duncan MK. Lens epithelial cells initiate an inflammatory response following cataract surgery. *Invest Ophthalmol Vis Sci*. 2018;59:4986-4997.
  86. Zindel J, Kubes P. DAMPs, PAMPs, and LAMPs in immunity and sterile inflammation. *Annu Rev Pathol*. 2019;15(1):493-518.
  87. Streilein JW. Ocular immune privilege: therapeutic opportunities from an experiment of nature. *Nat Rev Immunol*. 2003;3:879-889.
  88. Ransohoff RM, Engelhardt B. The anatomical and cellular basis of immune surveillance in the central nervous system. *Nat Rev Immunol*. 2012;12:623-635.

**How to cite this article:** DeDreu J, Bowen CJ, Logan CM, et al. An immune response to the avascular lens following wounding of the cornea involves ciliary zonule fibrils. *The FASEB Journal*. 2020;34:9316–9336. <https://doi.org/10.1096/fj.202000289R>